© 2025. Published by The Company of Biologists | Journal of Experimental Biology (2025) 228, jeb249422. doi:10.1242/jeb.249422

RESEARCH ARTICLE

How lacertids resolve spatial details: visual acuity in the common wall lizard (*Podarcis muralis*)

Anna Kawamoto[1,*], Guillem Pérez i de Lanuza[1], David Vie Giner[2], Jindřich Brejcha[3] and Enrique Font[1]

ABSTRACT

Visual acuity, the ability to discern static spatial details, is crucial for understanding how organisms perceive their environment. Lacertid lizards are diurnal, feed on small prey, and communicate using multiple visual signals, including postures, dynamic displays and conspicuous colour patches. However, their visual acuity remains unstudied, leaving a critical gap in our understanding of their visual capabilities. Visual acuity is often estimated behaviourally using an optomotor apparatus, which quantifies a reflex-orienting movement called the optomotor response (OMR), or histologically by evaluating retinal ganglion cell (RGC) densities. We combined these two techniques to estimate visual acuity in a lacertid lizard, *Podarcis muralis*. OMR assays estimated an acuity of 2.05 cpd, while RGC counts revealed a peak density (>7000 cells mm^{-2}) within the area centralis, corresponding to 1.56 cpd. RGC topographic maps revealed additional areas of high cell density in the dorso-nasal and dorso-temporal regions, while the area centralis was located slightly ventrally in the centro-temporal retina. This RGC distribution suggests adaptations to resolve stimuli in the centre and lower parts of the lizard's visual field, which may enhance predator and prey detection on the ground. Using our estimated acuities, we calculated that a lizard can detect a conspecific from 10 m and a 2 mm-long object from 40 cm away. In addition, we generated AcuityView images (R package) showing how this species might discern conspecific colour patches at different distances. These images suggest that beyond 10 cm, the surroundings become increasingly blurred, suggesting a role for static visual signals specifically in close-range communication.

KEY WORDS: Eye, Spatial resolution, Optomotor apparatus, Retinal ganglion cell, Vision, Visual signal

INTRODUCTION

Vision allows organisms to gather information from their surroundings and is crucial for communication, navigation, foraging, prey detection and predator avoidance (Smythe, 1975; Endler, 1978; Cronin et al., 2014). The efficacy of vision depends on a complex concert of intrinsic and extrinsic factors that can influence visual perception (Kohn, 2007). Because vision relies on the projection of an object's image onto the retina, its effectiveness is constrained by ocular parameters such as the typology of the eye (i.e. camera, mirror or compound), eye shape and size, pupil shape and size, and the type, size and density of photoreceptors (Kelber et al., 2003; Cronin et al., 2014; Feller et al., 2021; Fleishman, 2024). Extrinsic factors also constrain vision. Indeed, ecological variables such as the light environment (Caves et al., 2016, 2023; Warrant et al., 2020), the complexity of the visual scene (de Busserolles et al., 2014; Caves et al., 2017), the distance between the viewer and the visual stimulus (Coimbra and Manger, 2016), as well as aspects such as foraging mode, diet composition and mobility (Caves et al., 2024), play a relevant role in visual perception. Animals have accordingly evolved specialised visual systems reflecting their evolutionary history, behaviour and ecological context (Lythgoe, 1979; Hart, 2001; Hall, 2008; Osorio and Vorobyev, 2008; Cronin et al., 2014; Thomas et al., 2020; Caves et al., 2023, 2024; Fleishman, 2024).

One important aspect of visual perception is visual acuity. Visual acuity is defined as the ability to resolve spatial details in a visual scene (Cronin et al., 2014; Caves et al., 2018), and shows striking variation by orders of magnitude across organisms (Caves et al., 2018; Heukamp et al., 2020). Knowledge of visual acuity reveals the extent of the visual information that organisms can extract from their environment and can contribute significantly to an understanding of their behaviour and ecology. Many animals employ complex visual signals for communication (Hailman, 1977; Bradbury and Vehrencamp, 2011), the effectiveness of which strongly depends on the visual capabilities of the receivers. As the ability to resolve signal details is contingent upon the receiver's visual acuity, the receiver's sensory system plays a significant role in shaping the characteristics of visual signals, thereby serving as a critical determinant of signal design (Endler, 1992). Subtle, fine-scale visual signals and communication over long distances suggest that some species have remarkable visual acuity. However, research has seldom addressed this aspect of visual communication. Instead, it has focused on other aspects, such as receptor sensitivity and threshold or temporal resolution, which have been extensively explored in visual ecology (e.g. Fleishman et al., 1997; da Silva Souza et al., 2011; Cronin et al., 2014; Caves et al., 2016; Matsuo et al., 2021).

Various techniques, including behavioural, electrophysiological, anatomical and histological methods, have been used to assess visual acuity across multiple taxa, providing insights into these limiting factors and their variation among species. The axial length and the position of the nodal point of the eye determine the size of an image on the retina: the larger an image, the greater the number of photoreceptor cells it will cover, allowing greater spatial detail to be perceived. The radius of curvature of the eye and the density of photoreceptor cells determine the spatial details that can be extracted from this image (Cronin et al., 2014; Caves et al., 2018). In many eyes, each retinal ganglion cell (RGC) receives input from several photoreceptor cells, which increases sensitivity but reduces acuity (Caves et al., 2018). Acuity is thus ultimately limited by the image

[1]Ethology Lab, Cavanilles Institute of Biodiversity and Evolutionary Biology, University of Valencia, APDO 22085, 46071 València, Spain. [2]Institut de Ciència dels Materials, University of Valencia, APDO 22085, 46071 València, Spain. [3]Department of Philosophy and History of Sciences, Faculty of Science, Charles University in Prague, Viničná 7, 212000 Prague, Czech Republic.

*Author for correspondence (annakaw423@gmail.com)

A.K., 0000-0002-7691-0663; G.P.i.d.L., 0000-0003-3736-6957; D.V.G., 0000-0002-4018-2836; J.B., 0000-0002-2164-6375; E.F., 0000-0002-5115-0055

Received 12 August 2024; Accepted 22 March 2025

Journal of Experimental Biology (2025) 228, jeb249422. doi:10.1242/jeb.249422

size on the retina, the density of photoreceptors and the ratio of ganglion cells to photoreceptor cells. A high density of RGCs typically favours high visual acuity (Lee and Stevens, 2007; Rutowski et al., 2009). While a large eye is often associated with high acuity (i.e. greater axial length; e.g. Kirschfeld, 1976; Land and Nilsson, 2012; Hall, 2008; Caves et al., 2018), this is not universally the case. In many nocturnal species, large eyes, pupils and lenses are adaptations for increased light sensitivity rather than high resolution (Caves et al., 2018, 2023, 2024). These adaptations include larger photoreceptor cells and/or a higher degree of convergence onto ganglion cells, which enhance vision in low light but may reduce acuity. The presence of specific retinal specialisations with a high RGC density, such as a visual streak, a fovea or other high-density areas (e.g. area centralis) also favours a high visual acuity (Hughes, 1977; Masseck et al., 2008; Coimbra and Manger, 2016; Potier et al., 2017; Costa et al., 2020; Heukamp et al., 2020). The presence of these retinal specialisations and their distribution in a concentric or elongated manner across the retinal meridian (e.g. de Busserolles et al., 2014; Caves et al., 2021) provide valuable insights into a species' visual behaviour and ecology (Hauzman et al., 2018; Caves et al., 2017, 2018, 2024; Baden et al., 2020).

Behavioural tests, including operant conditioning experiments and measurement of optomotor or optokinetic responses, are frequently used to evaluate visual acuity (e.g. Bartol et al., 2002, 2003; Masseck et al., 2008; Ben-Simon et al., 2012; Caves et al., 2016, 2021; Lev-Ari et al., 2017; Parker et al., 2017). The optomotor response (OMR) is a reflexive head or body-orienting movement elicited by a global shift in the surrounding visual field (normally resulting from head or body movement). When it occurs naturally, it compensates for and stabilises the visual image change that results from self-motion. This reflex can be elicited using an optomotor apparatus and does not require any training. An optomotor apparatus, also called an 'optomotor drum', consists of a rotating cylinder with black and white vertical stripes on its inner wall, and a central platform where the animal to be tested is placed. The visual acuity threshold of a species can be evaluated by manipulating parameters such as stripe width, contrast between adjacent stripes, luminance and drum rotation angular velocity (Caves et al., 2020). Visual acuity is expressed in cycles per degree (cpd), which refers to the number of pairs of black and white stripes an organism can discriminate within a single degree of visual angle (Caves et al., 2020). The higher the cpd value, the greater the visual acuity. The optomotor apparatus has been mainly employed for studying fish, arthropods and some mammals to analyse contrast sensitivity, temporal and spatial visual acuity, visual performance between mutants, and inter- or intra-specific variation (see table S2 in Caves et al., 2020).

Visual acuity remains a relatively neglected parameter in work with reptiles, with extremely valuable but limited investigations focusing on a few lizard clades (Hayes and Ireland, 1972; Ireland and Gans, 1977; Ireland, 1979; Northmore and Granda, 1991; Bartol et al., 2002, 2003; Baker et al., 2007; Fleishman et al., 2017, 2020; Levi-Ari et al., 2017; Nagloo et al., 2019). Yet, many lizards feed on small, fast-moving prey and rely heavily on visual communication (e.g. Desfilis et al., 2003; Font et al., 2010; Fleishman and Font, 2019; Fleishman, 2024), making the exploration of their visual system essential for understanding their behaviour and ecology. Lizards have a rich repertoire of visual signals, including dynamic (i.e. movement-based) displays such as head bobs, foot shakes, various tail movements and dewlap extension (Carpenter and Ferguson, 1977; Cooper, 2001; Peters and Evans, 2003; Jenssen et al., 2005; Labra et al., 2007; Font et al., 2012a), as well as chromatic signals (e.g. Stapley and Whiting, 2006; Fleishman et al., 1993, 2011, 2017, 2020; Pérez i de Lanuza et al., 2014; Martin et al., 2015; Fleishman and Font, 2019). Lacertid lizards (Squamata: Lacertidae), in particular, display a wide range of dynamic and static visual signals (Weber, 1957; Verbeek, 1972; Edsman, 1990; Font et al., 2012a; Abalos et al., 2024), often featuring conspicuous lateral and ventrolateral colour patches that function as chromatic signals (Molina-Borja et al., 2006; Salvador and Veiga, 2008; Font et al., 2009; Pérez i de Lanuza et al., 2014; Names et al., 2019; Badiane and Font, 2021). Although previous studies have investigated colour vision and spectral sensitivity in some lacertids (e.g. Pérez i de Lanuza and Font, 2014; Martin et al., 2015; Pérez i de Lanuza et al., 2018), no research has yet explored how they visually discern spatial details.

The European common wall lizard, *Podarcis muralis*, is a small lacertid that relies on vision and visual stimuli for many aspects of its biology. While numerous studies have specifically investigated this species' colour perception and discrimination (e.g. Pérez i de Lanuza et al., 2014, 2018), no attention has been devoted to its visual acuity. *Podarcis muralis* has a diurnal activity, a preference for relatively open habitats, preys on small and often fast-moving prey, and is capable of detecting large predators at considerable distances (Font et al., 2012a). While chemical stimuli are important in male–male and male–female interactions, vision also plays an essential role in social interactions (Font et al., 2012a,b). Territorial behaviour in *Podarcis* males may partially rely on the ability to visually detect and recognise rivals from a distance (López and Martín, 2002; Font et al., 2012b). In common with other *Podarcis* species, males and, to a lesser extent, females of *P. muralis* possess conspicuous ultraviolet (UV)–blue patches on some of the outer ventral scales (OVS), each ca. 2 mm long. These conspicuous patches are typically displayed during social interactions, and prior studies have suggested that they may function as signals of individual quality, providing information about fighting ability in the course of male–male interactions (e.g. Pérez i de Lanuza et al., 2014). Many of these blue patches reflect in the UV wavelength range with a single peak of reflectance around 370 nm (Pérez i de Lanuza et al., 2014; Pérez i de Lanuza and Font, 2015).

Here, we estimated the visual acuity of *P. muralis* using a multidisciplinary approach involving a behavioural assessment using an optomotor apparatus to obtain OMR data, and a histological analysis to determine RGC density and distribution in their retina. Additionally, we used software to generate representative images of what the species is capable of resolving based on the estimated visual acuity.

MATERIALS AND METHODS

Lizard maintenance

Podarcis muralis (Laurenti 1768) used in this study were captured by noosing in Llívia (Cerdanya, Eastern Pyrenees, Spain). Nine adult males were captured in September 2021, and ten adult females were captured in October 2022. Immediately after capture, we brought the lizards to the laboratory at the University of Valencia, measured them, and individually housed them in glass terraria (20×40×25 cm) with a layer of coconut fibre as substrate, a water dish and a shelter. Terraria were illuminated with daylight fluorescent tubes (Reptistar 5.0, 6500 K), and a 30 W infrared (IR) heating bulb placed 30 cm above the substrate to provide additional illumination and a heating spot of ca. 32°C. Room temperature was maintained at 25°C from 10:00 h to 18:00 h and allowed to drop to 18°C at night, and the lighting was set to be on from 10:00 h to 17:00 h, to simulate photoperiod and temperature variation in the lizards' natural environment. All terraria were

Journal of Experimental Biology (2025) 228, jeb249422. doi:10.1242/jeb.249422

sprayed daily with water. Lizards were fed *Tenebrio molitor* larvae and small *Acheta domestica* 3 times weekly. Animals were released at the exact point of capture, previously georeferenced, when experiments were finished.

All procedures were conducted in accordance with the animal experimentation and care guidelines of the ABS/ASAB and received the approval of the institutional Ethics Committee of the University of Valencia (cod: 2018/VSC/PEA/0127). Lizards were captured and retained in the laboratory under permits SF/024/21, SF/0187/22, and SF/0165/24 provided by the Departament de Territori i Sostenibilitat (Generalitat de Catalunya).

Optomotor response

We constructed a 3D-printed optomotor apparatus (Caves et al., 2020), consisting of a static platform surrounded by a circular paper drum (diameter 360 mm, height 210 mm), and a programmable electric stepper motor allowing us to select the speed and direction of rotation. We placed a transparent polycarbonate cylinder in the centre (diameter 105 mm, height 165 mm) to restrain the animal's movements inside the apparatus. Stimuli were pairs of black and white stripes displayed on the inner wall of the paper drum. We calculated and adapted the width of our stripes from 1 to 10 cpd, according to the diameter of our drum and the native resolution of our printer (Caves et al., 2020). This range was selected based on reported visual acuity values in reptiles in the literature (e.g. Fleishman, 1992; New and Bull, 2011; Lev-Ari et al., 2017; Nagloo et al., 2019; Fleishman et al., 2020). Inaccurate alignments, incorrect width values of lines or low printer resolution can lead to distortions of the pattern when printing. To avoid Moiré patterns, we adjusted for all spatial frequencies and stripe widths to be whole number multiples of a dot size of 0.021 mm for a printer with a resolution of 1200 dpi (Table 1).

We tested ten spatial frequencies from 1 to 10 cpd, corresponding to different widths of single stripes, ranging from 1.418 to 0.127 mm (Table 1). This range allowed us to comprehensively explore visual acuity thresholds without bias toward specific spatial frequencies. A plain white drum without stripes was used as the control (0 cpd). The inside of the optomotor apparatus was illuminated with a non-flickering LED flashlight placed overhead, delivering a uniform illumination.

During experiments, we maintained a consistent drum speed of 2 rotations per minute (rpm), which is the lowest rotational speed that reliably elicits a strong OMR while minimising potential artefacts caused by excessively fast stimulus motion that could overwhelm or alter the natural tracking behaviour (Caves et al., 2021).

Table 1. Width of stripes for stimuli from 1 to 10 cycles per degree (cpd), adjusted for a printer with a resolution of 1200 dpi and considering a diameter of circular striped stimuli of 360 mm

		Width (mm)	
MSA	cpd	Single stripe	Stripe pair
1.73	1	1.418	2.836
3.41	2 (1.98)	0.720	1.439
5.27	3 (3.05)	0.466	0.931
6.82	4 (3.95)	0.360	0.720
8.28	5 (4.8)	0.296	0.593
10.54	6 (6.11)	0.233	0.466
11.60	7 (6.72)	0.212	0.423
14.50	8 (8.4)	0.169	0.339
16.56	9 (9.6)	0.148	0.296
19.32	10 (11.2)	0.127	0.254

MSA represents the minimum separable angle calculated considering the distance between the lizard's eyes and the stimulus. Stripe width was calculated based on whole-number multiples of the number of millimetres per dot the printer could produce and selected for stimuli (indicated in parentheses) matching the desired cpd as closely as possible.

From our optomotor drum measurements, we were able to calculate the minimum separable angle (MSA), corresponding to the stripe width used in a particular trial as:

$$\mathrm{MSA} = 2\arctan\left(\frac{0.5W}{\mathrm{RD}}\right), \quad (1)$$

where W represents stripe width and RD the reactive distance, which is the distance between the eyes of the tested animal and the stimuli (stripes) displayed on the drum wall, both in the same units.

We performed the experiment from 10:00 h to 18:00 h, 13–18 March 2022, for the nine males, and 21–26 November 2022, for the ten females. Each lizard was tested twice a day, with two spatial frequencies tested per day. Over 5 days, this systematic approach ensured that each animal was tested for all ten spatial frequencies. Each testing session lasted 2 min, during which four trials were conducted. Each trial lasted 30 s, with the drum's rotation direction alternating between clockwise and counterclockwise every 30 s. This resulted in two replicates for each rotation direction per spatial frequency tested per session.

Before each session, the experimental lizard was placed inside the transparent cylinder at the centre of the circular static platform of the optomotor apparatus and allowed to settle and acclimate to the apparatus and lighting conditions for 15 min. A 40 W incandescent lamp placed on top of the apparatus was turned on during this period to bring the lizards to their preferred body temperature (i.e. 32±2°C; Braña, 1991). The animal, spatial frequency, starting rotation direction and stimulus for each session were fully randomised using the *sample* function (Ripley, 1987; Becker et al., 1988) in R v.4.2.1 (http://www.R-project.org/) to avoid bias or order effects. Testing was conducted twice daily, with all individuals tested sequentially, once in the morning and once in the afternoon. This approach provided adequate rest between sessions to minimise habituation or fatigue and maintain the animals' engagement with the stimulus throughout the experiment. Behaviours were recorded using a GoPro video camera (EZVIZ SPORT S2) mounted above the apparatus, surrounded by an opaque circular disc with a central hole accommodating the camera lens. By employing video recording, we eliminated observer presence effects during trials, minimising potential bias and ensuring reproducible data collection. At the end of every session and before the next one, the transparent cylinder was thoroughly cleaned to eliminate any chemical cues from previous lizards.

A positive OMR was scored when a lizard moved its head following the rotating stimulus in the direction of the moving stimulus in at least two consecutive rotation reversals and ceased moving its head when the stimulus stopped rotating. Further, to adopt a conservative approach, we followed the criterion established by Caves et al. (2020), for which the acuity limit is the highest stimulus that elicited a positive OMR in at least three out of four trials within a session. Additionally, we recorded frequencies of other behaviours such as locomotion, wall scratching (escape attempts), tongue flicking and tail undulation (an antipredator behaviour, e.g. Font et al., 2012a), as well as the time elapsed from the beginning of drum rotation to the first OMR elicited (i.e. latency; Caves et al., 2020).

Analyses were done with R v.4.2.1 (http://www.R-project.org/). Because of our limited sample size and as assumptions of normality and homoscedasticity were not met (Shapiro–Wilk test and Levene's test, W=0.41 and F=18.98, respectively, P<0.001), OMRs were

compared between treatments (i.e. cpd stimuli) using non-parametric Fisher–Pitman permutation tests with *post hoc* Bonferroni–Holm correction (Holm, 1979). Comparisons of visual acuities between sexes were done with a non-parametric Mann–Whitney *U*-test. The significance threshold was set at $P<0.05$.

Histology and retinal ganglion cell topographic map distribution

We prepared six whole-mount retinas from the eyes of six adult males of *P. muralis*, coded PM0 to PM5. Of these eyes, five came from five individuals euthanised for a previous study (Andrade et al., 2019) and had been fixed in Karnovski's fixative and stored first in 0.1 mol l^{-1} phosphate buffer (PB) with 0.01% azide for several months and then for 5 years in regularly refreshed clean 0.1 mol l^{-1} PB. The sixth whole-mount retina was unfixed fresh tissue from an individual (PM0) euthanised for a separate study on lizard skin. We acclimated PM0 in the dark for 30 min, before using an overdose of ketamine HCl to euthanise it (Font and Schwartz, 1989). As soon as the animal ceased responding to pinching of the legs and tail, the head was removed, and the eyes were extracted from their orbits. All six eyeballs were cleared of surrounding tissues and immersed in a solution of 0.1 mol l^{-1} PB (pH 7.4) for 24 h. Using a microscale embedded in the microscope eyepiece, we measured each eye's axial length and marked the iris for dorsoventral orientation (i.e. transverse and axial lengths) before proceeding to the whole-mount preparation following the protocol described in Ullman et al. (2012). Briefly, once removed from the sclera, retinas underwent post-fixation in 4% paraformaldehyde in a PB solution 0.1 mol l^{-1}, then were stored in 0.1 mol l^{-1} PB with 0.01% azide for 48 h. We bleached the pigmented epithelium layer with a solution of 90 ml of 0.1 mol l^{-1} PB with 10 ml of 30% hydrogen peroxide and 80 ml of 1.0 mol l^{-1} potassium peroxide. We flattened specimens on gelatinised glass slides and dried them with 37% formalin vapour. We treated slides using xylene and absolute alcohol, then rehydrated the retinas with a series of descending alcohol concentrations before staining them with Nissl stain (0.1% Cresyl Violet). Subsequently, we rinsed our slides with distilled water and dehydrated the tissue with a series of ascending alcohol concentrations, to finally clear them in xylene before coverslipping with Permount mounting medium (Fisher Chemical).

As Nissl stain is not RGC specific and can also stain other cell types, such as amacrine and glial cells (Ullmann et al., 2012), we prepared retinal cross-sections for light and transmission electron microscopy (TEM) using standard procedures (Brejcha et al., 2019). This allowed for a detailed examination of the retinal layers and a thorough analysis of the constituent cell types (Fig. 1; Fig. S1). We used the right eye of PM0 and three additional right eyes from lizards euthanised, like PM0, for a separate study on lizard skin, all processed using the same protocol as the previously described whole-mount retina samples. TEM imaging provided high-resolution ultrastructural details, facilitating a more accurate cell- type identification and ensuring the recognition of RGCs in the other retinas (Fig. 2; Fig. S1). Glial cells are easily recognisable by their characteristic slender shape and relatively small size (Ehrlich, 1981). Amacrine cells are small, round cells with abundant Nissl substance, while ganglion cells have polygonal nuclei and larger soma that stain irregularly (Ullmann et al., 2012; de Busserolles et al., 2014; Costa et al., 2020).

To estimate the density of RGCs, we followed the mapping cell distribution method using an eyepiece graticule (Ullmann et al., 2012). The retinas were observed under a wide-field microscope (Nikon Eclipse E-800). In addition to brightfield illumination, we also took advantage of the auto-fluorescence of the samples (FITC 3540C, excitation 482 nm, emission 536 nm), which allowed us to distinguish the RGC layer more clearly by reducing interference from the underlying neural tissue layers. The fluorescent light parameters enhance cell boundary contrast and clarity, allowing for clear cell identification, even in densely packed regions (Fig. 2). Micro-photographs were captured using a digital camera associated with the microscope and the software NIS-Element B.R v. 5.21.03 (Nikon). We sampled around 200 sites per retina, employing a counting grid of 295×295 µm and a frame of 75×75 µm to ensure a Schaeffer coefficient of error (CE) below 0.1 (Glaser and Wilson, 1998), which was sufficient to capture the key trends and specialisations in the retinas. We conducted additional samplings within the area of higher cell density close to the conus papillaris, using a 25×25 µm counting frame with the same grid. The topographic distribution of RGCs was assessed using the optical fractionator method (West et al., 1991) (Table 2). Digital images were imported into ImageJ 1.53k (Schneider et al., 2012) for marking and counting cells. Using InkScape v.1.1 (The Inkscape Project Developer Team 2004; https://inkscape.org/id/release/inkscape-1.1.1/) we drew each retina's outline and isodensity lines to construct topographic maps of RGC density.

When estimating visual acuity based on anatomical data, calculations consider RGC peak density and posterior nodal distance (PND), which is the distance from the centre of the lens to the retina (i.e. two-thirds of the axial length; Pettigrew et al., 1988). We obtained a retinal magnification factor (RMF) of 0.0327 mm deg^{-1} calculated as:

$$\mathrm{RMF} = \frac{2\pi \mathrm{PND}}{360}, \tag{2}$$

which allowed us to calculate the Nyquist limits (f_N) of spatial resolving power (SRP) (Snyder and Miller, 1977; Coimbra and Manger, 2016; Nagloo et al., 2019) as follows:

$$f_N = 0.5 \times \mathrm{RMF} \times \left(\frac{2D}{\sqrt{3}}\right)^{1/2}, \tag{3}$$

where D represents the peak RGC density, in cells per mm^2.

AcuityView and minimum visual detection distance

We used the R package AcuityView (Caves and Johnsen, 2018) to estimate how visual acuity affects visual perception of the small ventrolateral motifs (i.e. UV–blue patches) of *P. muralis* by conspecifics. This package uses Fourier methods and considers the animal's visual acuity, the size of an observed object and the distance that separates them. We chose a picture of the UV–blue patches of a male *P. muralis*. Photographs were taken with a digital camera (Olympus PEN Mini). We generated images showing how the UV–blue patches would be perceived under varying visual acuities and viewing distances. Each image was resized to dimensions of 1024×1024 pixels to ensure compatibility with AcuityView (Caves and Johnsen, 2018). We conducted analyses at two distinct viewer distances: 0.1 and 1 m, and for five different levels of visual acuity: 1, 2, 10 and 60 cpd (the latter representing human visual acuity; Campbell and Green, 1965; da Silva Souza et al., 2011; Cronin et al., 2014).

We explored minimum visual detection distance depending on an object's size to relate our estimated visual acuity values with their behavioural significance (Coimbra and Manger, 2016), and obtain representative cases (e.g. object sizes such as for an average flank length of an adult lizard of 50 mm, or an average UV–blue patch of

Journal of Experimental Biology (2025) 228, jeb249422. doi:10.1242/jeb.249422

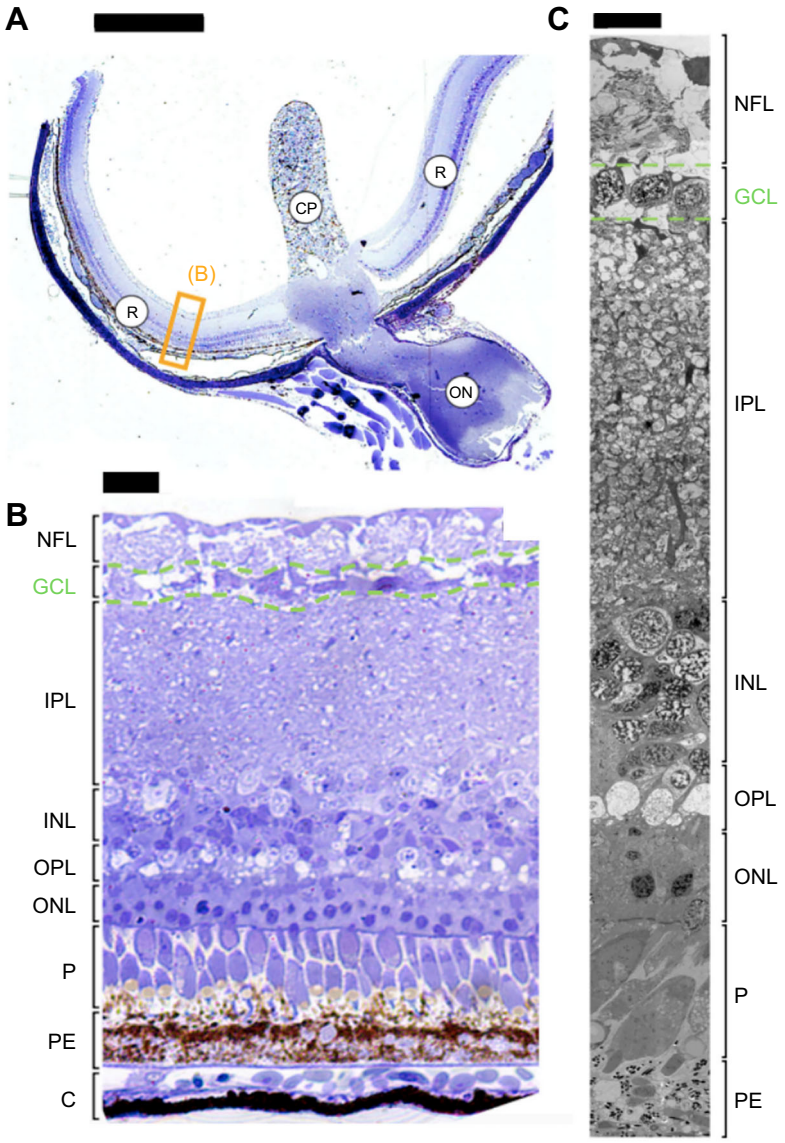

Fig. 1. Nissl-stained cross-section of a *Podarcis muralis* retina. (A) Semithin section of the retina. Scale bar: 500 µm. (B) The region indicated by the orange rectangle in A, at higher magnification. Scale bar: 50 µm. (C) The same region under transmission electron microscopy (TEM). Scale bar: 10 µm. CP, conus papillaris; R, retina; ON, optic nerve; NFL, nerve fibre layer (axons); GCL, ganglion cell layer; IPL, inner plexiform layer; INL, inner nuclear layer (amacrine, bipolar and horizontal cells); OPL, outer plexiform layer; ONL, outer nuclear layer; P, photoreceptors; PE, pigmented epithelium; C, choroid.

2 mm), following the formula:

$$d = \frac{\text{obj}}{\tan(\text{MRA})},$$

where d represents the minimum detection for an object of a given size (obj) and MRA is the minimum resolvable angle, representing the smallest angular distance at which a detail can be resolved on the retina, calculated as the inverse of the SRP divided by two (Gaffney and Hodos, 2003; Hodos et al., 2012; Coimbra and Manger, 2016; Coimbra et al., 2019).

RESULTS

Optomotor response

All lizards showed at least one OMR (i.e. head movement in the direction of the moving stripes) in some of the trials. Lizards exhibited OMRs at spatial frequencies between 1 and 10 cpd, although these were more frequent during trials involving 1–2 cpd. All lizards displayed positive OMRs in all four trials during the sessions involving 1 cpd (Fig. 3; Movie 1). Considering the positive response criterion set by Caves et al. (2020), we estimated an acuity of approximately 2 cpd for this species (n=19; mean±s.d.=2.053±1.649 cpd; median=1 cpd; range=1–7 cpd) (Fig. 3), with no differences between sexes (Z=−1.9046, P=0.057).

The frequency of OMRs significantly varied depending on the stimulus presented to the lizards (χ^2=153.47, P<0.0001). Lizards displayed a high frequency of this behaviour during trials involving the lowest spatial frequency of 1 cpd (mean±s.d.=36.42±16.66 OMRs; Z=3.972, P<0.0001), significantly decreasing at 2 cpd (mean±s.d.=2.74±4.08 OMRs; P<0.0001) (Fig. 4). Similarly, OMRs were induced right after triggering the drum rotation for 1 cpd, while we observed a significant latency for stimuli of higher value (mean±s.d.=3.59±2.48 s; χ^2=110.19, P<0.001). The mean (±s.d.) latency for 2 cpd was 8.57±4.72 s (Z=−3.805, P>0.06) (Fig. 4). From 2 to 10 cpd, there was no statistical difference in the mean of elicited OMRs or in the elapsed time until the first OMR was recorded (P=0.12). We did not observe a significant difference in the frequency of other behaviours depending on the stimulus (P>0.2). Finally, the peak of recorded OMRs corresponded to a width of a single stripe of 1.418 mm. Considering the parameters of the optomotor apparatus, we obtained a MSA of 0.578 deg equivalent to 1.732 cpd.

Journal of Experimental Biology (2025) 228, jeb249422. doi:10.1242/jeb.249422

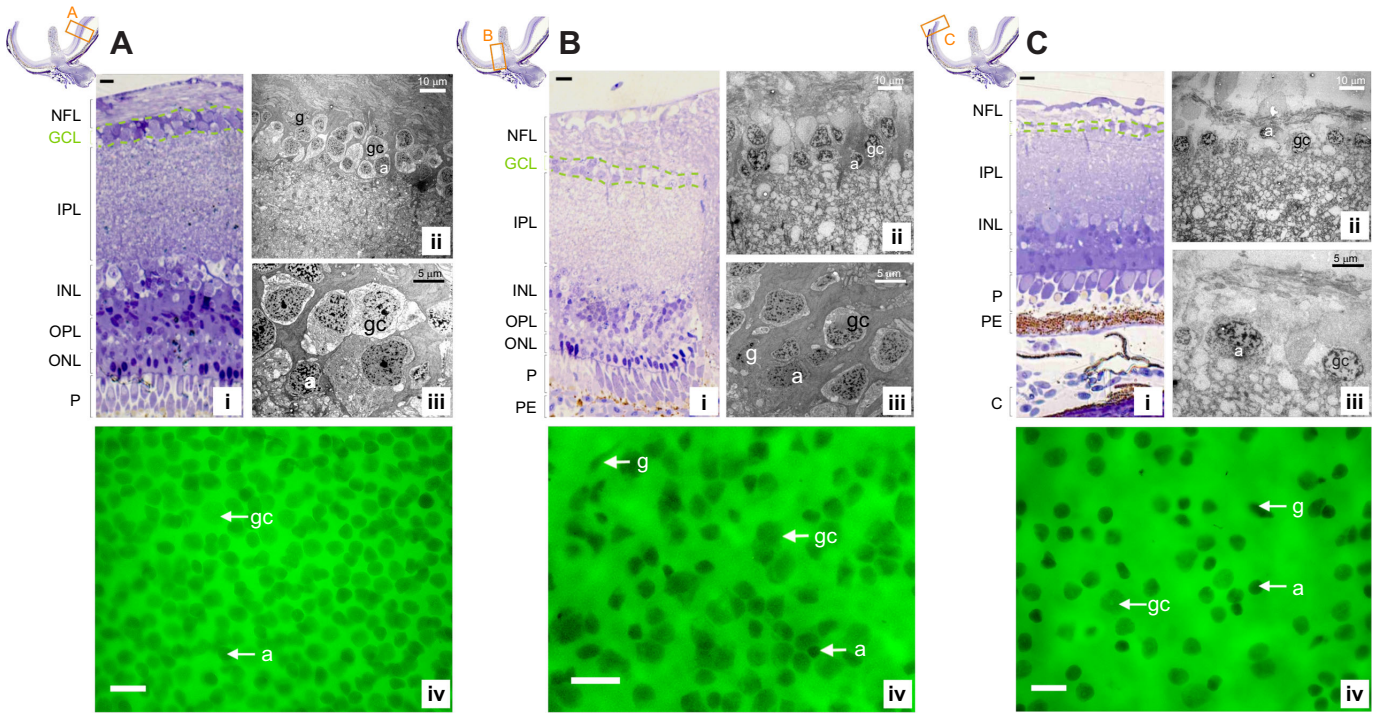

Fig. 2. *Podarcis muralis* retinal ganglion cell (RGC) regions using different imaging techniques. The figure illustrates three retinal regions (indicated by the orange rectangles in the respective panels) showing a high (A), medium (*conus papillaris*; B) and low (peripheral region; C) density of RGCs (peripheral region). (i) Semithin cross-sections of Nissl-stained retinas under light microscopy. Scale bars: 10 µm. (ii,iii) Ultrastructural details of cross-sectioned retinas under TEM. Scale bars: 10 µm (ii) and 5 µm (iii). (iv) Longitudinal views of the RGC layer under fluorescence microscopy. Scale bars: 10 µm. Retinal structures are identified as: NFL, nerve fibre layer (axons); GCL, ganglion cell layer; IPL, inner plexiform layer; INL, inner nuclear layer (amacrine cells, bipolar cells and horizontal cells); OPL, outer plexiform layer; ONL, outer nuclear layer; P, photoreceptors; PE, pigmented epithelium; and C, choroid. Specific cell types are labelled: gc, ganglion cell; a, amacrine cell; and g, glial cell.

RGC topographic distribution

Brightfield and fluorescence microscopy, as well as TEM, enabled us to distinguish between amacrine, glial and ganglion cells (Figs S1 and S2). Table 2 shows results of the optical fractionator method. Topographic maps revealed a heterogeneous distribution of RGC density in *P. muralis* retinas (Fig. 5). All individuals presented a region in the centro-temporal part of their retina with an increased density of RGCs, identified as an area centralis. However, localised artefacts during tissue processing, such as uneven flattening or minor distortions, may occasionally affect the accuracy of identifying valid regions of cell density concentration. In the case of PM2, such artefacts were observed, and the topography was excluded to ensure consistency with the overall pattern observed in the remaining retinas (Fig. 5).

RGC density peaks ranged from 3333 to 7322 cells mm^{-2} (n=6 retinas, mean±s.d.=5666±999 cells mm^{-2}) corresponding to spatial resolving powers from 1.16 to 1.56 cpd (Table 2). In addition, smaller concentric areas exhibiting high RGC densities were also identified in the dorso-nasal and dorso-temporal regions (Fig. 5).

AcuityView and minimum visual detection distance

The images generated using AcuityView (Fig. 6) suggest that *P. muralis* has limited visual resolution at distances over 1 m. The small UV–blue patches remain discernible, and each patch appears

Table 2. Summary of the stereological parameters established using the optical fractionator method to assess the density of ganglion cells and build the topographic distribution map of retinas in *Podarcis muralis*

Individual	AL (mm)	Total sampled retinal area (mm^2)	Counting grid size (µm)	Counting frame size (µm)	Objective/numerical aperture	Site no.	CE	Peak RGC density (cells mm^{-2})	Estimated VA (cpd)
PM0	2.9	19.1	295×295	75×75	100×/1.3 oil 40×/0.75 air	148	0.077	7322	1.56
PM1	3.3	18.7	295×295	75×75	100×/1.3 oil 40×/0.75 air	200	0.076	5000	1.47
PM2	3.0	16.8	295×295	75×75	100×/1.3 oil 40×/0.75 air	184	0.069	6018	1.46
PM3	3.1	18.2	295×295	75×75	100×/1.3 oil 40×/0.75 air	224	0.064	6342	1.55
PM4	3	15.6	295×295	75×75	100×/1.3 oil 40×/0.75 air	244	0.069	5979	1.46
PM5	3.2	15.8	295×295	75×75	100×/1.3 oil 40×/0.75 air	220	0.083	3333	1.16

AL, axial length; CE, Schaeffer's coefficient of error; RGC, retinal ganglion cells; VA, visual acuity; cpd, cycles per degree.

Journal of Experimental Biology (2025) 228, jeb249422. doi:10.1242/jeb.249422

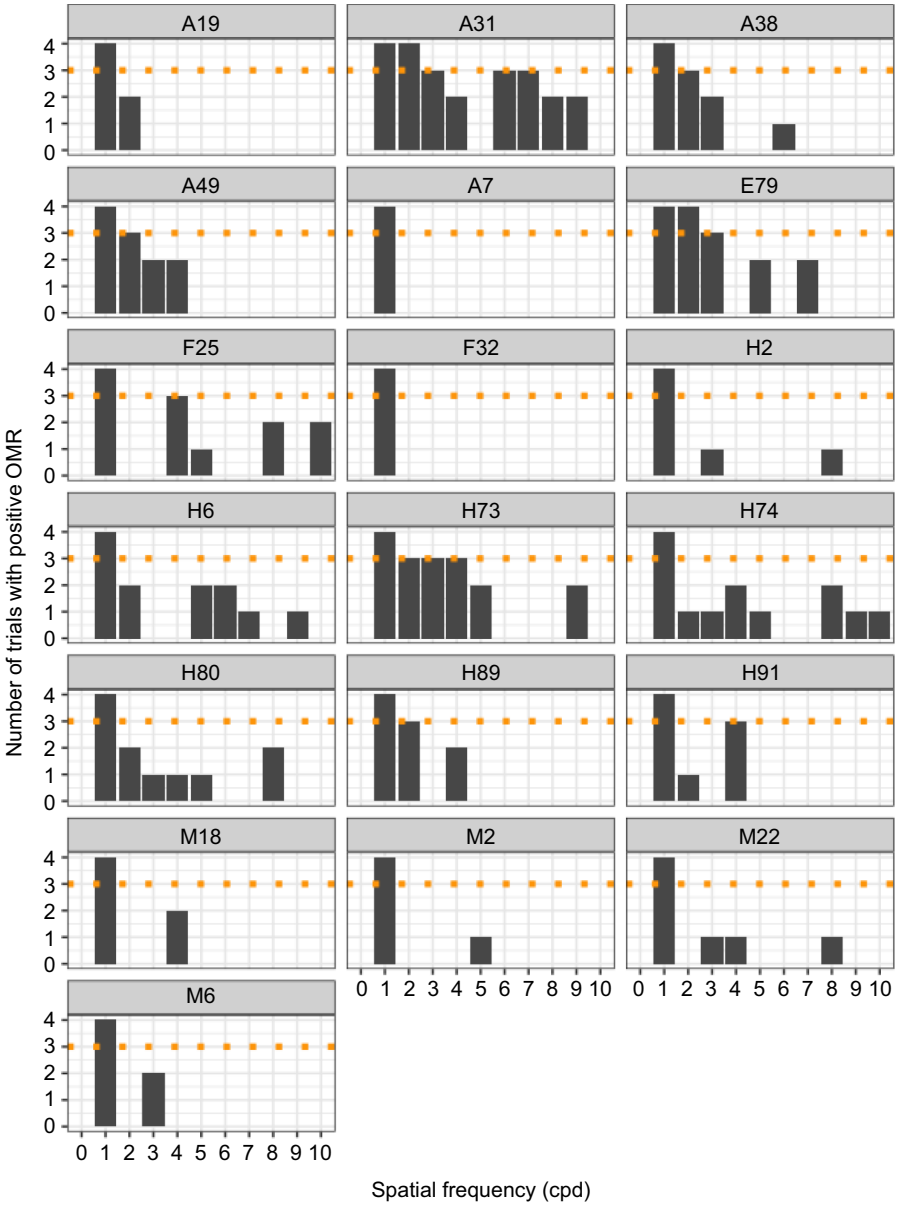

Fig. 3. Number of trials with a positive optomotor response (OMR) for each tested individual. Data are plotted against spatial frequency (cycles per degree, cpd). The dotted orange line shows the criterion used by Caves et al. (2020), i.e. the highest stimulus that elicited a positive OMR in at least three trials out of four.

distinguishable from the others at a distance of 0.1 m. An isolated 2 mm-long object, such as a single UV–blue patch or a small insect, should be detected at a distance of 40 cm. Under optimal light and contrast conditions, *P. muralis* lizards should be able to detect each other from 9.7 m.

DISCUSSION

Visual acuity affects the ability of an animal to detect biologically relevant objects in its environment and to resolve fine spatial details and patterns. Here, we report the first measurement of visual acuity in a lacertid lizard, which was obtained through two different procedures that provide similar estimates. Our behavioural experiment estimated a visual acuity for *P. muralis* averaging 2.05 cpd. Retinal topographic maps unveiled areas with a high density of RGCs, including an area centralis in the centro-temporal region housing a peak density of RGCs corresponding to an acuity averaging 1.56 cpd. Additionally, smaller areas of high RGC density were observed in the dorso-nasal and dorso-temporal regions.

The topographic distribution of RGCs reveals much about an animal's visual ecology (e.g. de Busserolles et al., 2014; Caves et al., 2021, 2024). Horizontal streaks, characterised by an increased density of RGCs along the naso-temporal axis of the retina, enhance a sharper panoramic visual field and are commonly found in animals living in open environments (e.g. coral reef fish, red kangaroo, arctic fox) (Collin and Pettigrew, 1988a; de Busserolles et al., 2014; Baden et al., 2020; Caves et al., 2021). Animals living in complex environments often present an area in their retina that is particularly dense in RGCs, allowing them to focus on objects accurately (Walls, 1942; Collin, 1999). A fovea is a pit or depression characterised by a displacement of inner retinal layers leading to a high density of ganglion cells and cone receptors (Provis et al., 2013). This structural modification reduces light scattering and allows enhanced spatial resolution, particularly in species requiring high-acuity vision. Likewise, an area centralis, although lacking this pit structure, features a localised concentric increase in photoreceptor and RGC density, improving resolution in a specific region of the visual field – a feature regularly encountered in

Journal of Experimental Biology (2025) 228, jeb249422. doi:10.1242/jeb.249422

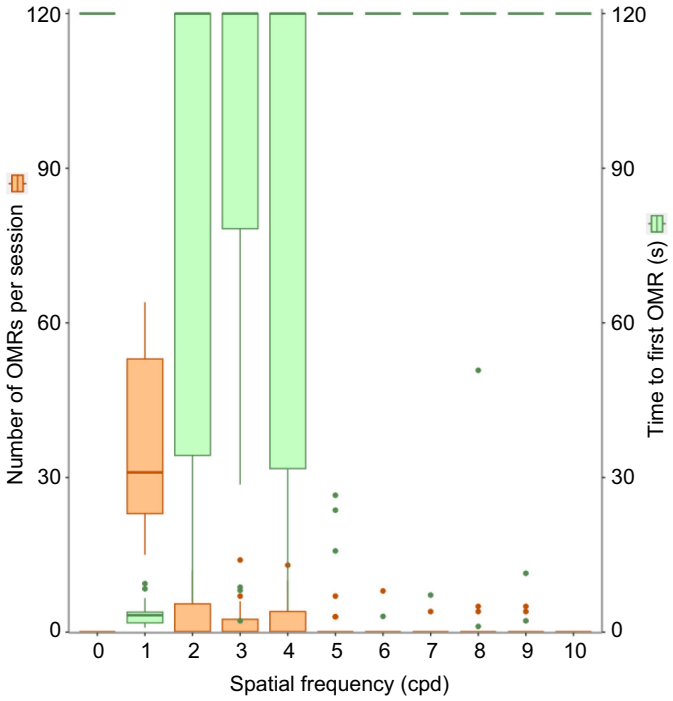

Fig. 4. Boxplots showing the number of optomotor responses and elapsed time until the first optomotor response was recorded per trial against spatial frequency (cpd). Trials lasted 120 s. The top and the bottom of the box represent, respectively, the 75th and 25th percentiles; the bold line represents the median. Dots represent outliers and extreme values.

predatory species (Hughes, 1977; Provis et al., 2013). The presence of an area centralis in the centro-temporal region of the *P. muralis* retina should enhance visual resolution in the central visual field by providing higher magnification and image stabilisation. This might increase the perception of fine details, potentially improving, for instance, the capture of small prey during hunting (Fite and Lister, 1981). Similarly, the additional small areas highly dense in RGCs in the dorso-temporal and dorso-nasal regions may enhance the perception of objects located on the ground, improving the detection of conspecifics and potential prey in the lower-front and lower-back areas of the visual field.

Wall lizards, especially territorial males, tend to occupy elevated perching sites, such as prominent rocks or other elevated objects, which they use as vantage points that allow them to scan the environment below and around them (Fig. 7) (Avery et al., 1993). The areas of high density of RGCs in the dorsal retina may enhance visual detection of objects located in the lower visual field when lizards adopt this scan posture and suggest an advantage in maintaining territory, locating food and scanning the environment below. Our minimum detection distance calculations indicate that *P. muralis* can detect an object the size of a conspecific from nearly 10 m. This finding agrees with field observations, where interactions between animals have been noted at distances spanning the size of their home ranges, which can extend up to 30 m (e.g. Boag, 1973; Edsman, 1990; Abalos et al., 2020). While most interactions (male–male, male–female) occur at close range, lizards seem capable of detecting conspecifics (e.g. territorial intruders) and responding to other individuals from afar.

Our findings provide insight into how far a receiver could detect a static communicative signal (i.e. signal active space) and other stimuli. *Podarcis muralis* should be able to resolve small prey (e.g. insects and spiders) or small chromatic signals such as the ventrolateral UV–blue patches (Abalos et al., 2024) within moderate ranges of less than 50 cm. However, factors beyond visual acuity, including differential responses to specific wavelengths and motion perception, may influence visual detection (Fleishman, 1986, 1992; Fleishman et al., 1993, 2011; Nava et al., 2009; Fleishman and Pallus, 2010; Pallus et al., 2010; Fleishman and Font, 2019). For instance, the UV reflectance of the UV–blue patches probably makes them more conspicuous to the lizard compared with a similarly sized insect. Moreover, a moving stimulus often leads to higher visual acuity than a stationary one (Fleishman, 1986; Fleishman et al., 2017). The acuity inferred from the OMRs may reflect the involvement of a visual pathway optimised for reflexive responses to broad spatial patterns, as opposed to the fine-detail discrimination required for object detection and other higher-order visual tasks. In both laboratory and field settings, *Podarcis* are particularly responsive to moving stimuli, whether they involve predators, prey or conspecifics (Desfilis et al., 1993, 2003). They also react to subtle, low-amplitude movements such as those used during foot shakes and head bobs (Font et al., 2012a). In contrast to static acuity, dynamic visual acuity depends on the contrast between a moving stimulus and its background, and relies on motion-sensitive cells in the visual cortex, especially in the magnocellular pathway (Fleishman and Persons, 2001; Fleishman and Pallus, 2010; Pallus et al., 2010; Clark, 2011), processing moving objects quickly. Yet, stimulus movement generally impairs the ability to discern fine details, reducing visual acuity as the object's speed increases (Quevedo et al., 2018). Our estimated acuity values also do not consider fine discriminations but only minimum detection distances under optimal lighting and contrast conditions, disregarding the effect of background complexity, which can impair signal detection in the visual field (Robinson, 1966; Fleishman, 1992; Collin, 1999).

Signal efficacy hinges on the signal's design characteristics, the behaviour involved in its emission by the sender, and the receiver's sensory system (Endler, 1992). Males of *P. muralis* display their UV–blue lateral coloration to an approaching conspecific by means of a raised-body display, which consists of raising the body by extending the forearms and compressing the flanks (Kitzler, 1941; Verbeek, 1972; Weber, 1957; Abalos et al., 2016, 2020). This behaviour exposes a row of UV–blue patches, each averaging <2 mm in diameter, aligned along each flank and forming either a continuous or discontinuous line (Pérez i de Lanuza et al., 2014). Thus, observers would perceive an averaged spatial representation of the motif (Fleishman et al., 2017), meaning they may interpret the aggregate visual signal of these patches as a unified pattern rather than discrete, individual spots, potentially extending the detectability of the signal. Our AcuityView images illustrate the challenge *P. muralis* faces in perceiving details of the UV–blue patches over varying distances, with limited discriminability of these patches at short distances (10 cm), and complete blurring at longer distances (1 m). In addition, while colour is conspicuous at short distances, it tends to blur and match the background at longer distances (Fleishman and Persons, 2001; Barnett et al., 2018). Because of UV light scattering more in the air than light of longer wavelengths (Lythgoe, 1980; Loew, 1996; Dong et al., 2013), the signal active space of these patches may be limited to shorter distances than those of chromatic signals in the human-visible spectrum, underscoring the role of these chromatic signals in close-range communication.

We reviewed the available literature on visual acuity in reptiles, recalculating values if necessary to ensure methodological consistency (see Table S1). Available estimates of lizard visual acuity vary widely

Journal of Experimental Biology (2025) 228, jeb249422. doi:10.1242/jeb.249422

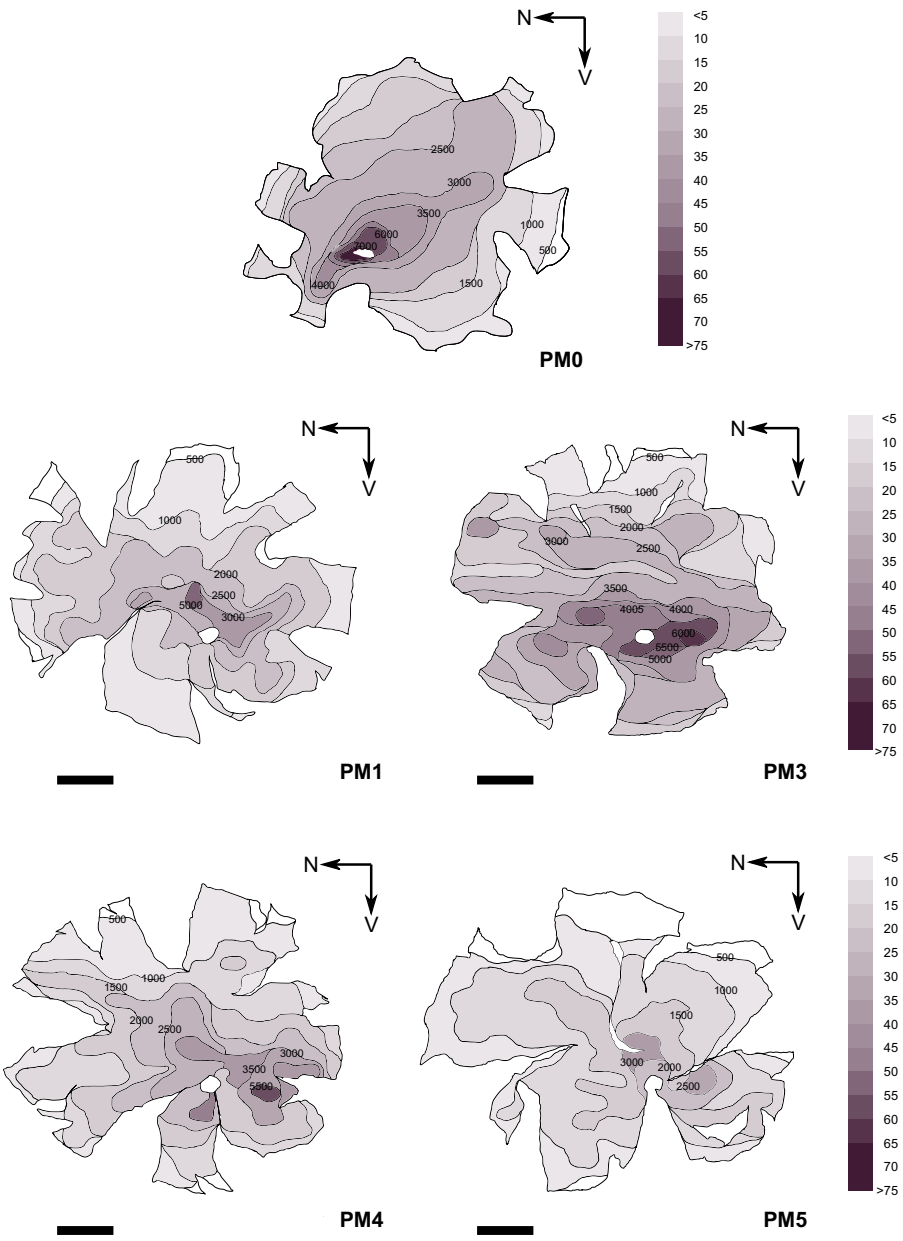

Fig. 5. Topographic maps representing the distribution of RGCs in the retina of five individuals (PM0, PM1, PM3, PM4 and PM5). Isodensity line values are shown every 500 cells mm^{-2}, and the colorimetric gradient of cell density values is in ×10^2 cells mm^{-2}. Arrows indicate the orientation of the retinas (N, nasal; V, ventral). Scale bars: 1 mm.

(*n*=14 lizard species; mean±s.d.=9.52±2.77 cpd; median=8.47 cpd; range=7.02–14.2 cpd) (Fig. 8; Fig. S2). This diversity is accompanied by an extraordinary variation in visual signals, from subtle, low amplitude behavioural displays and/or colour patches to large, highly conspicuous dynamic displays (e.g. Font and Kramer, 1989; Decourcy and Jenssen, 1994; Cooper and Frederick, 2007; Font et al., 2012a), intricately tied to each species' lifestyle and ecological requirements (Ott, 2005; Kelber and Roth, 2006; Coimbra and Manger, 2016; Thomas et al., 2020). Large variation in visual acuity values has similarly been reported in other groups, mainly driven by differences in eye size and ecology (e.g. birds; Caves et al., 2024).

Our findings indicate that the estimated acuity of *P. muralis* matches predictions based on the relationship between acuity and eye axial length (e.g. Veilleux and Kirk, 2014; Caves et al., 2017, 2018) and is consistent with values observed in other squamate species (Fig. 8). For instance, *Tiliqua rugosa* has an axial length of 9.3 mm (New and Bull, 2011) – over 3 times larger than that of *P. muralis* – and exhibits an accordingly higher visual acuity. However, the correlation between visual acuity and axial length is not always straightforward, with extrinsic factors exerting a significant influence. Environmental light, for instance, plays a pivotal role in shaping ocular features such as axial length and pupil size, ultimately impacting visual acuity. According to the resolution–sensitivity trade-off, larger eyes can prioritise sensitivity over acuity rather than necessarily enhancing acuity (Caves et al., 2023, 2024; Fleishman, 2024). Compared with diurnal geckos of the same eye and body size, nocturnal geckos and other lizard species living under low light conditions have large pupils and short focal lengths (Kelber and Roth, 2006), which results in a smaller image for a given axial length and, consequently, lower visual acuity (Röll, 2001).

Visual acuity in *Anolis* lizards has garnered significant attention. Most *Anolis* species have a dewlap, a foldable gular flap with varying colours and patterns, and exhibit highly conspicuous dynamic visual displays (e.g. push-ups, head bobs) in social contexts (Font and Kramer, 1989; Cook et al., 2013; Driessens et al.,

Journal of Experimental Biology (2025) 228, jeb249422. doi:10.1242/jeb.249422

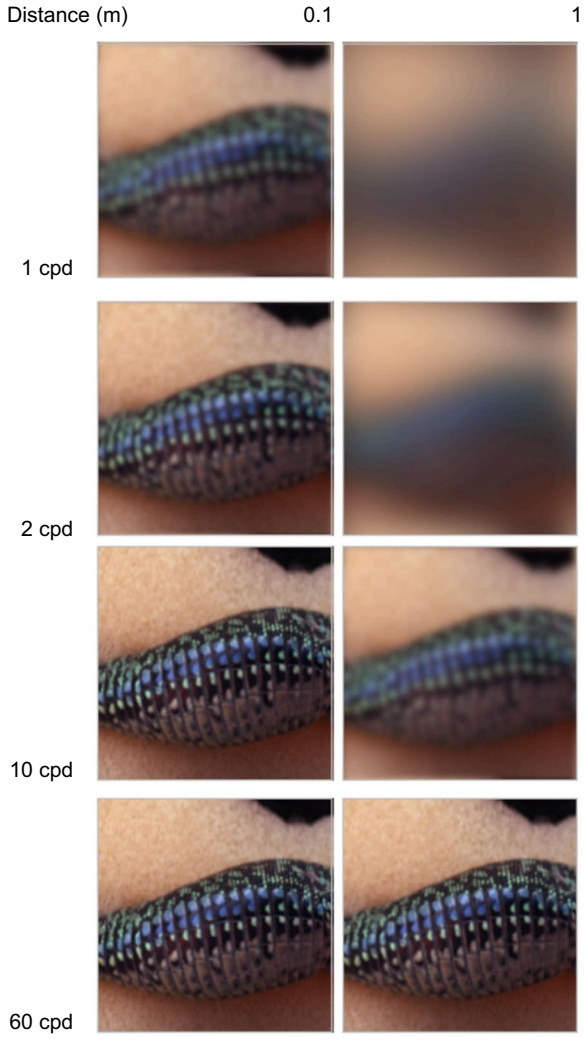

Fig. 6. Estimated view using AcuityView of the UV–blue patches on the outer ventral scales of a male *P. muralis*. Generated pictures were modelled at 0.1 and 1 m of the distance between the scene and the viewer, for visual acuities of 1, 2, 10 and 60 cpd (i.e. human), assuming the entire row of UV–blue patches is 5 cm long.

2015). Their well-developed visual system, adept at motion perception (Fleishman, 1986, 1992; Fleishman and Pallus, 2010; Pallus et al., 2010; Fleishman et al., 2017), and unique double fovea (i.e. a central and a temporal one; Makaretz and Levine, 1980; Fite and Lister, 1981), grant them the highest visual acuity recorded among lizards. Their sit-and-wait predatory strategy, long-range signalling and arboreal lifestyle in complex environments have probably driven the evolution of this high acuity visual system (Moermond, 1981; Fleishman, 1992; Arnold, 1998; Steinberg et al., 2014; Steinberg and Leal, 2016). Unlike *Podarcis*, which capture prey using jaw prehension, *Anolis* employ lingual prehension, requiring binocular fixation and precise depth perception for accurate tongue projection (Bels and Goosse, 1990; Schwenk, 2000). *Anolis carolinensis* boasts a maximum visual acuity of 12.5 cpd within its fovea, while peripheral acuity is 10 times lower (~1.25 cpd) (Fleishman et al., 2020). The peripheral acuity of *A. sagrei* ranges from 1.18 to 1.22 cpd depending on lighting conditions (Fleishman et al., 2017). This variation emphasises how visual resolution is context dependent, being higher for centrally focused objects and those at close range, while resolution diminishes

Fig. 7. Picture of a male *P. muralis* scanning its environment on top of a rock. Photo credit: Enrique Font.

in peripheral vision or at longer distances. The visual grasp reflex shifts peripheral images to the central fovea to enhance detail. Although *A. carolinensis* has an axial length 1.5 times that of *P. muralis*, its prominent convex cornea and highly mobile spheroid eyes (Rasys et al., 2021) adapted for dynamic tracking differ from *P. muralis*'s recessed, oblate eyes adapted to semi-open habitats. These structural differences probably reflect adaptations to their respective habitats and shape the visual capabilities of each species. *Anolis* lizards stand apart from most diurnal lizards, raising questions about the extent to which their adaptations can be considered to represent the typical lizard. While the dual foveal system and visual grasp reflex of *Anolis* probably evolved for predatory efficiency, *Podarcis* lizards are second to none in their ability to capture small, fast-moving prey, suggesting that a bifoveate retina is not a prerequisite for successfully tracking and capturing swift prey.

High visual acuity has also been reported in five *Ctenophorus* species (Agamidae) (Nagloo et al., 2019). Although we recalculated the published acuities considering peak RGC densities rather than photoreceptor densities to ensure consistency and comparability with other studies (Fig. 8), the estimated visual acuities for these species remain among the highest observed in reptiles, ranging from 6.76 to 9.88 cpd. Fig. S2 shows the original visual acuity values reported in the literature without recalculation. RGC topographies reveal that *Ctenophorus* possess a fovea and a horizontal streak (Nagloo et al., 2019). The high visual acuities and retinal specialisations observed in *Ctenophorus* imply potential advantages tailored to their ground-dwelling lifestyle in expansive landscapes, more vast areas and sparsely vegetated terrain than the semi-open habitats in which *P. muralis* evolved (Arnold, 1998).

Overall, these results highlight the litany of factors affecting visual acuity in lizards, including habitat type, life-history traits and specific ecological requirements. The relatively low visual acuity of *P. muralis* compared with that of *Anolis* and *Ctenophorus* lizards may reflect a trade-off in its visual system, prioritising field coverage and sensitivity over spatial resolution, shaped by various environmental factors related to its ground-dwelling lifestyle in relatively vegetated and saxicolous environments, such as boulders and rocks (Arnold, 1998). However, the interpretation of these acuity values remains challenging because of the intricate interplay of these influencing factors.

Journal of Experimental Biology (2025) 228, jeb249422. doi:10.1242/jeb.249422

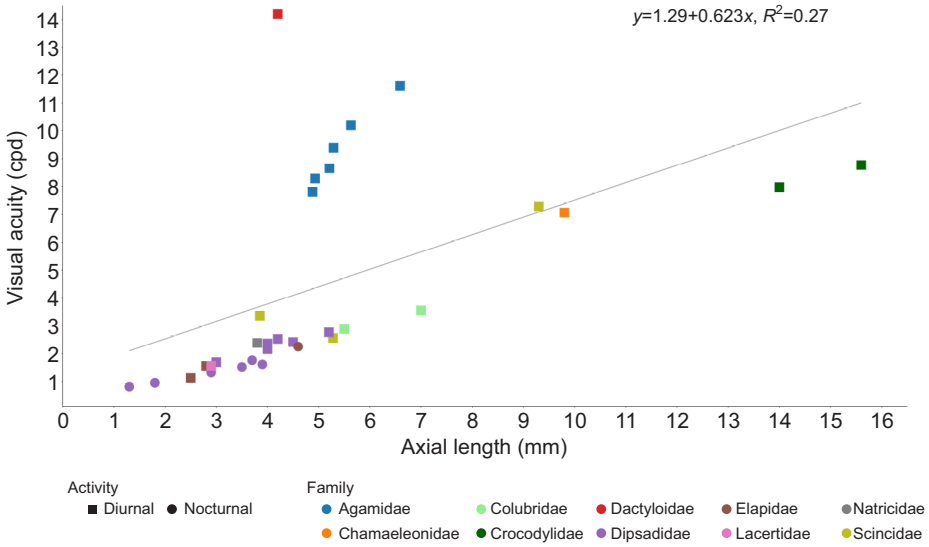

Fig. 8. Visual acuity relative to axial length across reptile families. Each dot represents the mean visual acuity estimated histologically in a species, published in previous papers. Acuity, peak RGC density, axial length, spatial resolution calculations, activity and their references can be found in Table S1.

There is a sizeable amount of literature on the visual system of lacertids from a neuroanatomical perspective, covering topics such as neural pathways, neuronal types and neurotransmitters (e.g. Medina and Smeets, 1992; Lanuza et al., 1996; Romero-Alemán et al., 2012). However, there is a notable gap in our knowledge regarding the anatomy and function of their eyes. This lack of detailed information on the visual apparatus leaves a significant area of their sensory biology unexplored, underscoring the need for further studies on lacertid eyes. Prior research in this area has been limited, with only one study suggesting the existence of a shallow central fovea in *Podarcis liolepis* (formerly *Podarcis hispanica*; Lanuza et al., 1996), which probably corresponds to an area centralis, as observed in *P. muralis* in the present study. The low visual acuity of *P. muralis* relative to other species might reflect this species' unique ecological, morphological and physiological adaptations. Our approach using both behavioural and cell count estimates yielded congruent results, and the 0.5 cpd discrepancy between the two estimates falls within the range of individual variability. External factors may produce biased results (Abdeljalil et al., 2005), but in our case, the inclusion of a control enabled us to minimise these potentially confounding effects. Although we estimated the acuity of *P. muralis* at 2 cpd using a threshold criterion (≥75% response) (Caves et al., 2020, 2021), some lizards responded to spatial frequencies of up 10 cpd. Responses elicited at higher spatial frequencies were scattered and probably driven by experimental artefacts rather than stimulus perception. These artefacts include subtle shadows or reflections from uneven illumination, minor vibrations or motor noise generated by the optomotor apparatus during stimulus rotation, and slight micro-irregularities at the seam where stimulus sheets were joined. In contrast, the analysis of OMR frequencies and latencies revealed markedly higher occurrences and prompt elicitation of OMRs at 1 cpd compared with higher spatial frequencies, strongly supporting an acuity limit of *P. muralis* between 1 and 2 cpd. A refined spaced set of spatial frequencies near the acuity threshold could yield a more detailed response curve and warrants future exploration.

It is worth noting that the eyes that had been stored for several years proved effective for whole-mount preparation and subsequent RGC analyses. This suggests that fresh tissue may not be required for whole-mount preparation. Challenges in distinguishing between RGCs and amacrine cells have been reported in previous studies (Ullmann et al., 2012), some of which categorised them all as neuronal cells (e.g. Hart, 2002; Theiss et al., 2007), which may have resulted in inflated values of visual acuity. Neuronal cells also exhibit variations depending on the species and their distribution across different regions of the retina (e.g. Hassni et al., 1997; Costa et al., 2020). In this regard, we leveraged the tissue's autofluorescence properties and the light-absorbing characteristics of Nissl-stained cells, which, unlike brightfield microscopy, minimised the visibility of layers beyond the focal plane and allowed precise localisation of cells of interest even in densely packed regions. Despite its prevalent use in most studies, Nissl staining may introduce artefacts that compromise sample quality (Ullmann et al., 2012), impeding cell visibility and identification (Collin and Pettigrew, 1988b). Future work may benefit from considering alternative staining procedures that are RGC specific, such as immuno-histochemistry and/or transcription factors (Haverkamp et al., 2021; DAPI: Pushchin, 2022; Pushchin and Aleskerov, 2024).

Altogether, our results should help mitigate anthropomorphic bias (Rivas and Burghardt, 2002; Caves et al., 2018; Brebner et al., 2024) when interpreting *P. muralis* behaviour, particularly considering that human visual acuity is estimated at 60 cpd compared with the 1.5–2 cpd acuity calculated here for *P. muralis*. Exploring the myriad factors influencing visual acuity in lizards reveals an intricate interplay of evolutionary, ecological, behavioural and physiological determinants. We believe our findings offer valuable insights into the visual capabilities of *P. muralis*, providing the first-ever values of visual acuity in a lacertid species and expanding our understanding of its sensory ecology.

Acknowledgements
We wish to express our gratitude to Dr José Manuel García Verdugo and his research group at the Cavanilles Institute, as well as to Mario Soriano Navarro for his expert support in transmission electron microscopy (TEM) at the Centro de Investigación Príncipe Felipe (CIPF) in Valencia. We gratefully acknowledge the use of the CIPF core microscopy facilities, whose resources and technical expertise in cell identification and imaging significantly contributed to the advancement of this study.

Competing interests
The authors declare no competing or financial interests.

Author contributions
Conceptualization: G.P.i.d.L., E.F.; Data curation: A.K.; Formal analysis: A.K.; Funding acquisition: G.P.i.d.L., E.F.; Investigation: A.K.; Methodology: A.K., J.B., D.V.G., E.F.; Resources: J.B., D.V.G., E.F.; Supervision: G.P.i.d.L., E.F.; Validation:

J.B., G.P.i.d.L., E.F.; Visualization: A.K., J.B.; Writing - original draft: A.K.; Writing - review & editing: A.K., J.B., D.V.G., G.P.i.d.L., E.F.

Funding
Fieldwork, experiments and preparation of this manuscript were supported by grants from the Spanish Ministerio de Ciencia e Innovación (PID2019-104721GB-I00) and the Generalitat Valenciana (AICO/2021/113) to E.F. and G.P.i.d.L.

Data and resource availability
All relevant data can be found within the article and its supplementary information.

ECR Spotlight
This article has an associated ECR Spotlight interview with Anna Kawamoto.

References

Abalos, J., Pérez i de Lanuza, G., Carazo, P. and Font, E. (2016). The role of male coloration in the outcome of staged contests in the European common wall lizard (*Podarcis muralis*). *Behaviour* **153**, 607-631. doi:10.1163/1568539X-00003366

Abalos, J., Pérez I De Lanuza, G., Bartolomé, A., Liehrmann, O., Laakkonen, H., Aubret, F., Uller, T., Carazo, P. and Font, E. (2020). No evidence for differential sociosexual behavior and space use in the color morphs of the European common wall lizard (*Podarcis muralis*). *Ecol. Evol.* **10**, 10986-11005. doi:10.1002/ece3.6659

Abalos, J., Pérez I De Lanuza, G., Bartolomé, A., Liehrmann, O., Aubret, F. and Font, E. (2024). Behavioral threat and appeasement signals take precedence over static colors in lizard contests. *Behav. Ecol.* **35**, arae045. doi:10.1093/beheco/arae045

Abdeljalil, J., Hamid, M., Abdel-Mouttalib, O., Stéphane, R., Raymond, R., Johan, A., José, S., Pierre, C. and Serge, P. (2005). The optomotor response: a robust first-line visual screening method for mice. *Vision Res.* **45**, 1439-1446. doi:10.1016/j.visres.2004.12.015

Andrade, P., Pinho, C., Pérez I De Lanuza, G., Afonso, S., Brejcha, J., Rubin, C.-J., Wallerman, O., Pereira, P., Sabatino, S. J., Bellati, A. et al. (2019). Regulatory changes in pterin and carotenoid genes underlie balanced color polymorphism in the wall lizard. *Proc. Natl Acad. Sci. USA* **116**, 5633-5642. doi:10.1073/pnas.1820320116

Arnold, E. N. (1998). Structural niche, limb morphology and locomotion in lacertid lizards (Squamata: Lacertidae), a preliminary survey. *Bull. Natu. History Museum Lond.* **64**, 63-89.

Avery, R., Basker, A. and Corti, C. (1993). “Scan” behaviour in *Podarcis muralis*: the use of vantage points by an actively foraging lizard. *Amphib-Reptilia* **14**, 247-259. doi:10.1163/156853893X00444

Baden, T., Euler, T. and Berens, P. (2020). Understanding the retinal basis of vision across species. *Nat. Rev. Neurosci.* **21**, 5-20. doi:10.1038/s41583-019-0242-1

Badiane, A. and Font, E. (2021). Information content of ultraviolet-reflecting colour patches and visual perception of body coloration in the Tyrrhenian wall lizard *Podarcis tiliguerta*. *Behav. Ecol. Sociobiol.* **75**, 96. doi:10.1007/s00265-021-03023-2

Baker, R. A., Gawne, T. J., Loop, M. S. and Pullman, S. (2007). Visual acuity of the midland banded water snake estimated from evoked telencephalic potentials. *J. Comp. Physiol. A* **193**, 865-870. doi:10.1007/s00359-007-0240-z

Barnett, J. B., Michalis, C., Scott-Samuel, N. E. and Cuthill, I. C. (2018). Distance-dependent defensive coloration in the poison frog *Dendrobates tinctorius*, *Dendrobatidae*. *Proc. Natl Acad. Sci. USA* **115**, 6416-6421. doi:10.1073/pnas.1800826115

Bartol, S., Musick, J. A. and Ochs, A. L. (2002). Visual acuity thresholds of juvenile loggerhead sea turtles (*Caretta caretta*): an electrophysiological approach. *J. Comp. Physiol. A* **187**, 953-960. doi:10.1007/s00359-001-0262-x

Bartol, S. M., Mellgren, R. L. and Musick, J. A. (2003). Visual acuity of juvenile loggerhead sea turtles (*Caretta caretta*): a behavioral approach. *Int. J. Comp. Psychol.* **16**, 143-155. doi:10.46867/C4T601

Becker, R. A., Chambers, J. M. and Wilks, A. R. (1988). *The New S Language*. Computer Science Series, Pacific Grove, CA: Wadsworth & Brooks/Cole.

Bels, V. L. and Goosse, V. (1990). Comparative kinematic analysis of prey capture in *Anolis carolinensis* (Iguania) and *Lacerta viridis* (Scleroglossa). *J. Exp. Zool.* **255**, 120-124. doi:10.1002/jez.1402550116

Ben-Simon, A., Ben-Shahar, O., Vasserman, G., Ben-Tov, M. and Segev, R. (2012). Visual acuity in the archerfish: behavior, anatomy, and neurophysiology. *J. Vis.* **12**, 18. doi:10.1167/12.12.18

Boag, D. A. (1973). Spatial relationships among members of a population of wall lizards. *Oecologia* **12**, 1-13. doi:10.1007/BF00345467

Bradbury, J. W. and Vehrencamp, S. L. (2011). *Principles of Animal Communication*, 2nd edn. p. 768, Sunderland, MA: Sinauer.

Braña, F. (1991). Summer activity patterns and thermoregulation in the Wall lizard, *Podarcis muralis*. *Herpetol. J.* **1**, 544-549.

Brebner, J. S., Loconsole, M., Hanley, D. and Vasas, V. (2024). Through an animal’s eye: the implications of diverse sensory systems in scientific experimentation. *Pro. R. Soc. B* **291**, 20240022. doi:10.1098/rspb.2024.0022

Brejcha, J., Bataller, J. V., Bosáková, Z., Geryk, J., Havlíková, M., Kleisner, K., Maršík, P. and Font, E. (2019). Body coloration and mechanisms of colour production in Archelosauria: the case of deirocheline turtles. *R. Soc. Open Sci.* **6**, 190319. doi:10.1098/rsos.190319

Campbell, F. W. and Green, D. G. (1965). Optical and retinal factors affecting visual resolution. *J. Physiol.* **181**, 576. doi:10.1113/jphysiol.1965.sp007784

Carpenter, C. C. and Ferguson, G. W. (1977). Variation and evolution of stereotyped behavior in reptiles. *Biol. Reptil.* **7**, 335-554.

Caves, E. M. and Johnsen, S. (2018). AcuityView: An R package for portraying the effects of visual acuity on scenes observed by an animal. *Methods Ecol. Evol.* **9**, 793-797. doi:10.1111/2041-210X.12911

Caves, E. M., Frank, T. M. and Johnsen, S. (2016). Spectral sensitivity, spatial resolution and temporal resolution and their implications for conspecific signalling in cleaner shrimp. *J. Exp. Biol.* **219**, 597-608. doi:10.1242/jeb.122275

Caves, E. M., Sutton, T. T. and Johnsen, S. (2017). Visual acuity in ray-finned fishes correlates with eye size and habitat. *J. Exp. Biol.* **220**, 1586-1596. doi:10.1242/jeb.151183

Caves, E. M., Brandley, N. C. and Johnsen, S. (2018). Visual acuity and the evolution of signals. *Trends Ecol. Evol.* **33**, 358-372. doi:10.1016/j.tree.2018.03.001

Caves, E. M., Troscianko, J. and Kelley, L. A. (2020). A customizable, low–cost optomotor apparatus: A powerful tool for behaviourally measuring visual capability. *Methods Ecol. Evol.* **11**, 1319-1324. doi:10.1111/2041-210X.13449

Caves, E. M., de Busserolles, F. and Kelley, L. A. (2021). Sex differences in behavioural and anatomical estimates of visual acuity in the green swordtail, *Xiphophorus helleri*. *J. Exp. Biol.* **224**, jeb243420. doi:10.1242/jeb.243420

Caves, E. M., Sutton, T. T., Warrant, E. J. and Johnsen, S. (2023). Measures and models of visual acuity in epipelagic and mesopelagic teleosts and elasmobranchs. *J. Comp. Physiol. A* **209**, 807-826. doi:10.1007/s00359-023-01661-7

Caves, E. M., Fernández-Juricic, E. and Kelley, L. A. (2024). Ecological and morphological correlates of visual acuity in birds. *J. Exp. Biol.* **227**, jeb246063. doi:10.1242/jeb.246063

Clark, U. (2011). Magnocellular neurons. In *Encyclopedia of Clinical Neuropsychology* (ed. J. S. Kreutzer, J. DeLuca and B. Caplan). New York, NY: Springer.

Coimbra, J. P. and Manger, P. R. (2016). Retinal ganglion cell topography and spatial resolving power in the white rhinoceros (*Ceratotherium simum*). *J. Comp. Neurol.* **525**, 2484-2498. doi:10.1002/cne.24136

Coimbra, J. P., Alagaili, A. N., Bennett, N. C., Mohammed, O. B. and Manger, P. R. (2019). Unusual topographic specializations of retinal ganglion cell density and spatial resolution in a cliff-dwelling artiodactyl, the Nubian ibex (*Capra nubiana*). *J. Comp. Neurol.* **527**, 2813-2825.

Collin, S. (1999). Behavioural ecology and retinal cell topography. In *Adaptive Mechanisms in the Ecology of Vision*, Vol. 1 (ed. S. N. Archer, M. B. A. Djamgoz, E. R. Loew, J. C. Partridge,and S. Vallerga), pp. 509-535. Kluwer Academic Publishers.

Collin, S. P. and Pettigrew, J. D. (1988a). Retinal topography in reef teleosts: II. Some species with prominent horizontal streaks and high-density areae. *Brain Behav. Evol.* **31**, 283-295. doi:10.1159/000116595

Collin, S. P. and Pettigrew, J. D. (1988b). Retinal topography in reef teleosts: I. Some species with well-developed areae but poorly-developed streaks. *Brain Behav. Evol.* **31**, 269-282. doi:10.1159/000116594

Cook, E. G., Murphy, T. G. and Johnson, M. A. (2013). Colorful displays signal male quality in a tropical anole lizard. *Naturwissenschaften* **100**, 993-996. doi:10.1007/s00114-013-1095-5

Cooper, W. E. (2001). Multiple roles of tail display by the curly–tailed lizard *Leiocephalus carinatus*: pursuit deterrent and deflective roles of a social signal. *Ethology* **107**, 1137-1149. doi:10.1046/j.1439-0310.2001.00754.x

Cooper, W. E. and Frederick, W. G. (2007). Optimal flight initiation distance. *J. Theor. Biol.* **244**, 59-67. doi:10.1016/j.jtbi.2006.07.011

Costa, K. H. A., Gomes, B. D., Silveira, L. C. D. L., Souza, G. D. S., Martins, I. C. V. D. S., Lacerda, E. M. D. C. B. and Rocha, F. A. D. F. (2020). Ganglion cells and displaced amacrine cells density in the retina of the collared peccary (*Pecari tajacu*). *PLoS ONE* **15**, e0239719. doi:10.1371/journal.pone.0239719

Cronin, T. W., Johnsen, S., Marshall, N. J. and Warrant, E. J. (2014). *Visual Ecology*. Princeton University Press. 768 p.

Da Silva Souza, G., Gomes, B. D. and Silveira, L. C. L. (2011). Comparative neurophysiology of spatial luminance contrast sensitivity. *Psychol. Neurosci.* **4**, 29-48. doi:10.3922/j.psns.2011.1.005

de Busserolles, F., Marshall, N. J. and Collin, S. P. (2014). Retinal ganglion cell distribution and spatial resolving power in deep-sea lanternfishes (*Myctophidae*). *Brain Behav. Evol.* **84**, 262-276. doi:10.1159/000365960

Decourcy, K. R. and Jenssen, T. A. (1994). Structure and use of male territorial headbob signals by the lizard *Anolis carolinensis*. *Anim. Behav.* **47**, 251-262. doi:10.1006/anbe.1994.1037

Desfilis, E., Font, E. and Gomez, A. (1993). An ethological study of feeding in the lizard, *Podarcis hispanica*. In *Lacertids of the Mediterranean Region: A Biological Approach* (ed. E. D. Valakos, W. Bohme, V. Perez-Mellado and P. Maragou), pp. 183-198. Hellenic Zoological Society.

Desfilis, E., Font, E. and Guillén-Salazar, F. (2003). Stimulus control of predatory behavior by the Iberian wall lizard (*Podarcis hispanica*, Sauria, Lacertidae): effects of familiarity with prey. *J. Comp. Psychol.* **117**, 309-316. doi:10.1037/0735-7036.117.3.309

Dong, J. Z., Lei, C., Zheng, X. J., Ai, X. R., Wang, Y. and Wang, Q. (2013). Light wavelengths regulate growth and active components of *Cordyceps militaris* fruit bodies. *J. Food Biochem.* **37**, 578-584. doi:10.1111/jfbc.12009

Driessens, T., Huyghe, K., Vanhooydonck, B. and Van Damme, R. (2015). Messages conveyed by assorted facets of the dewlap, in both sexes of *Anolis sagrei*. *Behav. Ecol. Sociobiol.* **69**, 1251-1264. doi:10.1007/s00265-015-1938-5

Edsman, L. (1990). Territoriality and competition in wall lizards. *PhD thesis*, Department of Zoology, University of Stockholm.

Ehrlich, D. (1981). Regional specialization of the chick retina as revealed by the size and density of neurons in the ganglion cell layer. *J. Comp. Neurol.* **195**, 643-657. doi:10.1002/cne.901950408

Endler, J. A. (1978). A predator's view of animal color patterns. In *Evolutionary Biology* (ed. M. K. Hecht, W. C. Steere and B. Wallace), pp. 319-364. Boston, MA: Springer US.

Endler, J. A. (1992). Signals, signal conditions, and the direction of evolution. *Am. Nat.* **139**, S125-S153. doi:10.1086/285308

Feller, K. D., Sharkey, C. R., McDuffee-Altekruse, A., Bracken-Grissom, H. D., Lord, N. P., Porter, M. L. and Schweikert, L. E. (2021). Surf and turf vision: Patterns and predictors of visual acuity in compound eye evolution. *Arthropod Struct. Dev.* **60**, 101002. doi:10.1016/j.asd.2020.101002

Fite, K. V. and Lister, B. C. (1981). Bifoveal vision in *Anolis* lizards. *Brain Behav. Evol.* **19**, 144-154. doi:10.1159/000121639

Fleishman, L. J. (1986). Motion detection in the presence and absence of background motion in an *Anolis* lizard. *J. Comp. Physiol. A* **159**, 711-720. doi:10.1007/BF00612043

Fleishman, L. J. (1992). The influence of the sensory system and the environment on motion patterns in the visual displays of anoline lizards and other vertebrates. *Am. Nat.* **139**, S36-S61. doi:10.1086/285304

Fleishman, L. J. (2024). Lizard visual ecology. *Front. Amphibian Reptile Sci.* **2**, 1426675. doi:10.3389/famrs.2024.1426675

Fleishman, L. J. and Font, E. (2019). Sensory processing in relation to signaling behavior. In *Behavior of Lizards: Evolutionary and Mechanistic Perspectives* (ed. V. Bels and A. Russell), pp. 207-258. Abingdon, UK: Taylor and Francis Publishing.

Fleishman, L. J. and Pallus, A. C. (2010). Motion perception and visual signal design in *Anolis* lizards. *Proc. R. Soc. B* **277**, 3547-3554. doi:10.1098/rspb.2010.0742

Fleishman, L. J. and Persons, M. (2001). The influence of stimulus and background colour on signal visibility in the lizard *Anolis cristatellus*. *J. Exp. Biol.* **204**, 1559-1575. doi:10.1242/jeb.204.9.1559

Fleishman, L. J., Loew, E. R. and Leal, M. (1993). Ultraviolet vision in lizards. *Nature* **365**, 397. doi:10.1038/365397a0

Fleishman, L. J., Bowman, M., Saunders, D., Miller, W. E., Rury, M. J. and Loew, E. R. (1997). The visual ecology of Puerto Rican anoline lizards: habitat light and spectral sensitivity. *J. Comp. Physiol. A* **181**, 446-460. doi:10.1007/s003590050128

Fleishman, L. J., Loew, E. R. and Whiting, M. J. (2011). High sensitivity to short wavelengths in a lizard and implications for understanding the evolution of visual systems in lizards. *Proc. R. Soc. B* **278**, 2891-2899. doi:10.1098/rspb.2011.0118

Fleishman, L. J., Yeo, A. I. and Perez, C. W. (2017). Visual acuity and signal color pattern in an *Anolis* lizard. *J. Exp. Biol.* **220**, 2154-2158. doi:10.1242/jeb.150458

Fleishman, L. J., Prebish, M. G. F. and Leal, M. (2020). The effects of limited visual acuity and context on the appearance of *Anolis* lizard dewlaps. *J. Herpetol.* **54**, 355-360. doi:10.1670/19-108

Font, E. and Kramer, M. (1989). A multivariate clustering approach to display repertoire analysis: headbobbing in *Anolis equestris*. *Amphib-Reptilia* **10**, 331-344. doi:10.1163/156853889X00476

Font, E. and Schwartz, J. M. (1989). Ketamine as an anesthetic for some squamate reptiles. *Copeia* **1989**, 484-486. doi:10.2307/1445448

Font, E., Pérez I De Lanuza, G. and Sampedro, C. (2009). Ultraviolet reflectance and cryptic sexual dichromatism in the ocellated lizard, Lacerta (*Timon*) lepida (Squamata: Lacertidae): UV coloration in the ocellated lizard. *Biol. J. Linn. Soc.* **97**, 766-780. doi:10.1111/j.1095-8312.2009.01251.x

Font, E., Carazo, P., Pérez I De Lanuza, G. and Barbosa, D. (2010). Comportamiento y comunicación animal: ¿Qué nos enseñan los lagartos? *Acta Zool. Lilloana* **54**, 11-34.

Font, E., Carazo, P., Pérez i de Lanuza, G. and Kramer, M. (2012a). Predator-elicited foot shakes in wall lizards (*Podarcis muralis*): evidence for a pursuit-deterrent function. *J. Comp. Psychol.* **126**, 87-96. doi:10.1037/a0025446

Font, E., Barbosa, D., Sampedro, C. and Carazo, P. (2012b). Social behavior, chemical communication, and adult neurogenesis: studies of scent mark function in *Podarcis* wall lizards. *Gen. Comp. Endocrinol.* **177**, 9-17. doi:10.1016/j.ygcen.2012.02.015

Gaffney, M. F. and Hodos, W. (2003). The visual acuity and refractive state of the American kestrel (*Falco sparverius*). *Vision Res.* **43**, 2053-2059. doi:10.1016/S0042-6989(03)00304-3

Glaser, E. M. and Wilson, P. D. (1998). The coefficient of error of optical fractionator population size estimates: a computer simulation comparing three estimators. *J. Microsc.* **192**, 163-171. doi:10.1046/j.1365-2818.1998.00417.x

Hailman, J. P. (1977). *Optical Signals: Animal Communication and Light*. Bloomington, IL: Indiana University Press, 362 p.

Hall, M. I. (2008). Comparative analysis of the size and shape of the lizard eye. *Zoology* **111**, 62-75. doi:10.1016/j.zool.2007.04.003

Hart, N. S. (2001). The visual ecology of avian photoreceptors. *Prog. Retin. Eye Res.* **20**, 675-703. doi:10.1016/S1350-9462(01)00009-X

Hart, N. S. (2002). Vision in the peafowl (Aves: *Pavo cristatus*). *J. Exp. Biol.* **205**, 3925-3935. doi:10.1242/jeb.205.24.3925

Hassni, M. E., M'Hamed, S. B., Repérant, J. and Bennis, M. (1997). Quantitative and topographical study of retinal ganglion cells in the chameleon (*Chameleo chameleon*). *Brain Res. Bull.* **44**, 621-625. doi:10.1016/S0361-9230(97)00285-2

Hauzman, E., Bonci, D. M. O. and Ventura, D. F. (2018). Retinal topographic maps: a glimpse into the animals' visual world. *Sens. Nervous System* **1**, 101-126. doi:10.5772/intechopen.74645

Haverkamp, S., Albert, L., Balaji, V., Němec, P. and Dedek, K. (2021). Expression of cell markers and transcription factors in the avian retina compared with that in the marmoset retina. *J. Comp. Neurol.* **529**, 3171-3193. doi:10.1002/cne.25154

Hayes, W. N. and Ireland, L. C. (1972). A study of visual orientation mechanisms in turtles and guinea pigs. *Brain Behav. Evol.* **5**, 226-239. doi:10.1159/000123749

Heukamp, A. S., Warwick, R. A. and Rivlin-Etzion, M. (2020). Topographic variations in retinal encoding of visual space. *Annu. Rev. Vision Sci.* **6**, 237-259. doi:10.1146/annurev-vision-121219-081831

Hodos, W., Lazareva, O. F., Shimizu, T. and Wasserman, E. (2012). What birds see and what they don't. In *How Animals See the World: Comparative Behavior, Biology, and Evolution of Vision* (ed. O. F. Lazareva, T. Shimizu,and E. A. Wasserman), pp. 5-24. Oxford University Press, Inc.

Holm, S. (1979). A simple sequentially rejective multiple test procedure. *Scand. J. Stat.* **6**, 65-70.

Hughes, A. (1977). The topography of vision in mammals of contrasting life style: comparative optics and retinal organisation. In *The Visual System in Vertebrates*, Vol. 7/5 (ed. F. Crescitelli). pp. 613-756. Handbook of Sensory Physiology. Berlin: Springer.

Ireland, L. C. (1979). Optokinetic behavior of the hatchling green turtle (*Chelonia mydas*) soon after leaving the nest. *Herpetologica* **35**, 365-370.

Ireland, L. C. and Gans, C. (1977). Optokinetic behavior of the tuatara, *Sphenodon punctatus*. *Herpetologica* **33**, 339-344.

Jenssen, T. A., Decourcy, K. R. and Congdon, J. D. (2005). Assessment in contests of male lizards (*Anolis carolinensis*): how should smaller males respond when size matters? *Anim. Behav.* **69**, 1325-1336. doi:10.1016/j.anbehav.2004.07.023

Kelber, A. and Roth, L. S. V. (2006). Nocturnal colour vision–not as rare as we might think. *J. Exp. Biol.* **209**, 781-788. doi:10.1242/jeb.02060

Kelber, A., Vorobyev, M. and Osorio, D. (2003). Animal colour vision - Behavioural tests and physiological concepts. *Biol. Rev.* **78**, 81-118. doi:10.1017/S1464793102005985

Kirschfeld, K. (1976). The resolution of lens and compound eyes. In *Neural Principles in Vision* (ed. F. Zettler and R. Weiler), pp. 354-370. Proceedings in Life Sciences. Berlin: Springer.

Kitzler, G. (1941). Die Paarungsbiologie einiger Eidechsen. *Z. Tierpsychol.* **4**, 353-402.

Kohn, A. (2007). Visual adaptation: Physiology, mechanisms, and functional benefits. *J. Neurophysiol.* **97**, 3155-3164. doi:10.1152/jn.00086.2007

Labra, A., Carazo, P., Desfilis, E. and Font, E. (2007). Agonistic interactions in a *Liolaemus* lizard: structure of head bob displays. *Herpetologica* **63**, 11-18. doi:10.1655/0018-0831(2007)63[11:AIIALL]2.0.CO;2

Land, M. F. and Nilsson, D. E. (2012). *Animal Eyes*, 2nd edn. Oxford Animal Biology Series. Oxford University Press, Inc.

Lanuza, E., Martinez-Marcos, A., Font, C. and Martinezgarcia, F. (1996). Catecholaminergic interplexiform cells in the retina of lizards. *Vision Res.* **36**, 1349-1355. doi:10.1016/0042-6989(95)00292-8

Lee, S. and Stevens, C. F. (2007). General design principle for scalable neural circuits in a vertebrate retina. *Proc. Natl Acad. Sci. USA* **104**, 12931-12935. doi:10.1073/pnas.0705469104

Lev-Ari, T., Katz, H. K., Lustig, A. and Katzir, G. (2017). Visual acuity and optokinetic directionality in the common chameleon (*Chamaeleo chamaeleon*). *EC Ophthalmol.* **6**, 145-154.

Loew, L. M. (1996). Potentiometric dyes: imaging electrical activity of cell membranes. *Pure Appl. Chem.* **68**, 1405-1409. doi:10.1351/pac199668071405

López, P. and Martín, J. (2002). Chemical rival recognition decreases aggression levels in male Iberian wall lizards, *Podarcis hispanica*. *Behav. Ecol. Sociobiol.* **51**, 461-465. doi:10.1007/s00265-001-0447-x

Lythgoe, J. N. (1979). *The Ecology of Vision*. Oxford Science Publications. Clarendon Press. University of California.

Lythgoe, J. N. (1980). Vision in fishes: ecological adaptations. In *Environmental Physiology of Fishes*, Vol. 35 (ed. M. A. Ali). NATO Advanced Study Institutes Series. Boston, MA: Springer.

Makaretz, M. and Levine, R. L. (1980). A light microscopic study of the bifoveate retina in the lizard *Anolis carolinensis*: general observations and convergence ratios. *Vision Res.* **20**, 679-686. doi:10.1016/0042-6989(80)90092-9
Martin, M., Le Galliard, J.-F., Meylan, S. and Loew, E. R. (2015). The importance of ultraviolet and near-infrared sensitivity for visual discrimination in two species of lacertid lizards. *J. Exp. Biol.* **218**, 458-465. doi:10.1242/jeb.115923
Masseck, O., Röll, B. and Hoffmann, K.-P. (2008). The optokinetic reaction in foveate and afoveate geckos. *Vision Res.* **48**, 765-772. doi:10.1016/j.visres.2007.12.004
Matsuo, M., Kamei, Y. and Fukamachi, S. (2021). Behavioural red-light sensitivity in fish according to the optomotor response. *R. Soc. Open Sci.* **8**, 210415. doi:10.1098/rsos.210415
Medina, L. and Smeets, W. J. A. J. (1992). Cholinergic, monoaminergic and peptidergic innervation of the primary visual centers in the brain of the lizards *Gekko gecko* and *Gallotia galloti*. *Brain Behav. Evol.* **40**, 171-181. doi:10.1159/000316110
Moermond, T. C. (1981). Prey-attack behavior of Anolis lizards. *Z. Tierpsychol.* **56**, 128-136. doi:10.1111/j.1439-0310.1981.tb01291.x
Molina-Borja, M., Font, E. and Mesa Avila, G. (2006). Sex and population variation in ultraviolet reflectance of colour patches in *Gallotia galloti* (Fam. *Lacertidae*) from Tenerife (Canary Islands). *J. Zool.* **268**, 193-206. doi:10.1111/j.1469-7998.2005.00008.x
Nagloo, N., Coimbra, J. P., Hoops, D., Hart, N. S., Collin, S. P. and Hemmi, J. M. (2019). Retinal topography and microhabitat diversity in a group of dragon lizards. *J. Comp. Neurol.* **528**, 542-558. doi:10.1002/cne.24780
Names, G., Martin, M., Badiane, A. and Le Galliard, J.-F. (2019). The relative importance of body size and UV coloration in influencing male-male competition in a lacertid lizard. *Behav. Ecol. Sociobiol.* **73**, 98. doi:10.1007/s00265-019-2710-z
Nava, S. S., Conway, M. A. and Martins, E. P. (2009). Divergence of visual motion detection in diurnal geckos that inhabit bright and dark habitats. *Funct. Ecol.* **23**, 794-799. doi:10.1111/j.1365-2435.2009.01565.x
New, S. T. D. and Bull, C. M. (2011). Retinal ganglion cell topography and visual acuity of the sleepy lizard (*Tiliqua rugosa*). *J. Comp. Physiol. A* **197**, 703-709. doi:10.1007/s00359-011-0635-8
Northmore, D. P. M. and Granda, A. M. (1991). Refractive state, contrast sensitivity, and resolution in the freshwater turtle, *Pseudemys scripta elegans*, determined by tectal visual-evoked potentials. *Vis. Neurosci.* **7**, 619-625. doi:10.1017/S0952523800010403
Osorio, D. and Vorobyev, M. (2008). A review of the evolution of animal colour vision and visual communication signals. *Vision Res.* **48**, 2042-2051. doi:10.1016/j.visres.2008.06.018
Ott, M. (2005). Visual accommodation in vertebrates: mechanisms, physiological response and stimuli. *J. Comp. Physiol. A* **192**, 97-111. doi:10.1007/s00359-005-0049-6
Pallus, A. C., Fleishman, L. J. and Castonguay, P. M. (2010). Modeling and measuring the visual detection of ecologically relevant motion by an *Anolis* lizard. *J. Comp. Physiol. A* **196**, 1-13. doi:10.1007/s00359-009-0487-7
Parker, A. N., Fritsches, K. A., Newport, C., Wallis, G. and Siebeck, U. E. (2017). Comparison of functional and anatomical estimations of visual acuity in two species of coral reef fish. *J. Exp. Biol.* **220**, 2387-2396. doi:10.1242/jeb.149575
Pérez I De Lanuza, G. and Font, E. (2014). Ultraviolet vision in lacertid lizards: Evidence from retinal structure, eye transmittance, SWS1 visual pigment genes, and behaviour. *J. Exp. Biol.* **217**, 2899-2909. doi:10.1242/jeb.104281
Pérez I De Lanuza, G. and Font, E. (2015). Differences in conspicuousness between alternative color morphs in a polychromatic lizard. *Behav. Ecol.* **26**, 1432-1446. doi:10.1093/beheco/arv075
Pérez I De Lanuza, G., Carazo, P. and Font, E. (2014). Colours of quality: Structural (but not pigment) coloration informs about male quality in a polychromatic lizard. *Anim. Behav.* **90**, 73-81. doi:10.1016/j.anbehav.2014.01.017
Pérez I De Lanuza, G., Ábalos, J., Bartolomé, A. and Font, E. (2018). Through the eye of a lizard: Hue discrimination in a lizard with ventral polymorphic coloration. *J. Exp. Biol.* **221**, jeb169565. doi:10.1242/jeb.169565
Peters, R. A. and Evans, C. S. (2003). Design of the Jacky dragon visual display: Signal and noise characteristics in a complex moving environment. *J. Comp. Physiol. A* **189**, 447-459. doi:10.1007/s00359-003-0423-1
Pettigrew, J. D., Dreher, B., Hopkins, C. S., McCall, M. J. and Brown, M. (1988). Peak density and distribution of ganglion cells in the retinae of microchiropteran bats: implications for visual acuity. *Brain Behav. Evol.* **32**, 48-56.
Potier, S., Mitkus, M., Bonadonna, F., Duriez, O., Isard, P.-F., Dulaurent, T., Mentek, M. and Kelber, A. (2017). Eye size, fovea, and foraging ecology in accipitriform raptors. *Brain Behav. Evol.* **90**, 232-242. doi:10.1159/000479783
Provis, J. M., Dubis, A. M., Maddess, T. and Carroll, J. (2013). Adaptation of the central retina for high acuity vision: cones, the fovea and the avascular zone. *Progress Retin. Eye Res.* **35**, 63-81. doi:10.1016/j.preteyeres.2013.01.005
Pushchin, I. (2022). Retinal ganglion cell distribution and spatial resolution in the Asiatic toad *Bufo gargarizans* (Günther, 1859). *Vision Res.* **195**, 107960. doi:10.1016/j.visres.2021.10.001
Pushchin, I. and Aleskerov, N. (2024). Retinal ganglion cell topography and spatial resolving power in the pajama cardinalfish S*phaeramia nematoptera* (Bleeker, 1856). *J. Fish Biol.* **104**, 1299-1307. doi:10.1111/jfb.15680
Quevedo, L., Aznar-Casanova, J. A. and Silva, J. A. D. (2018). Dynamic visual acuity. *Trends Psychol.* **26**, 1283-1297. doi:10.9788/TP2018.3-06En
Rasys, A. M., Pau, S. H., Irwin, K. E., Luo, S., Kim, H. Q., Wahle, M. A., Trainor, P. A., Menke, D. B. and Lauderdale, J. D. (2021). Ocular elongation and retraction in foveated reptiles. *Dev. Dyn.* **250**, 1584-1599. doi:10.1002/dvdy.348
Ripley, B. D. (1987). *Stochastic Simulation*. John Wiley & Sons.
Rivas, J. A. and Burghardt, G. M. (2002). Crotalomoprhism: a metaphor to understand anthropomorfism by omission. In *The Cognitive Animal: Empirical and Theoretical Perspectives on Animal Cognition* (ed. M. Bekoff, A., Colin and G. M. Burghardt), pp. 9-17. Cambridge: MIT Press.
Robinson, M. H. (1966). Anti-predator adaptations in stick and leaf-mimicking insects. *PhD thesis*, Oxford University, UK.
Röll, B. (2001). Retina of Bouton's skink (Reptilia, Scincidae): Visual cells, fovea, and ecological constraints. *J. Comp. Neurol.* **436**, 487-496. doi:10.1002/cne.1082
Romero-Alemán, M. M., Monzón-Mayor, M., Santos, E., Lang, D. M. and Yanes, C. (2012). Neuronal and glial differentiation during lizard (*Gallotia galloti*) visual system ontogeny. *J. Comp. Neurol.* **520**, 2163-2184. doi:10.1002/cne.23034
Rutowski, R. L., Gislén, L. and Warrant, E. J. (2009). Visual acuity and sensitivity increase allometrically with body size in butterflies. *Arthropod. Struct. Dev.* **38**, 91-100. doi:10.1016/j.asd.2008.08.003
Salvador, A. and Veiga, J. (2008). A permanent signal related to male pairing success and survival in the lizard *Psammodromus algirus*. *Amphib-Reptilia*, **29**, 117-120. doi:10.1163/156853808783431488
Schneider, C. A., Rasband, W. S. and Eliceiri, K. W. (2012). NIH Image to ImageJ: 25 years of image analysis. *Nat. Methods* **9**, 671-675. doi:10.1038/nmeth.2089
Schwenk, K. (2000). Feeding in lepidosaurs. In *Feeding: Form, Function, and Evolution in Tetrapod Vertebrates* (ed. K. Schwenk), pp. 175-291. Academic Press.
Smythe, R. H. (1975). *Vision in the Animal World*. London: Macmillan.
Snyder, A. W. and Miller, W. H. (1977). Photoreceptor diameter and spacing for highest resolving power. *JOSA* **67**, 696-698. doi:10.1364/JOSA.67.000696
Stapley, J. and Whiting, M. J. (2006). Ultraviolet signals fighting ability in a lizard. *Biol. Lett.* **2**, 169-172. doi:10.1098/rsbl.2005.0419
Steinberg, D. S. and Leal, M. (2016). Visual motion detection and habitat preference in Anolis lizards. *J. Comp. Physiol. A* **202**, 783-790. doi:10.1007/s00359-016-1120-1
Steinberg, D. S., Losos, J. B., Schoener, T. W., Spiller, D. A., Kolbe, J. J. and Leal, M. (2014). Predation-associated modulation of movement-based signals by a Bahamian lizard. *Proc. Natl Acad. Sci. USA* **111**, 9187-9192. doi:10.1073/pnas.1407190111
Theiss, S. M., Lisney, T. J., Collin, S. P. and Hart, N. S. (2007). Colour vision and visual ecology of the blue-spotted maskray, *Dasyatis kuhlii* Müller & Henle, 1814. *J. Comp. Physiol. A* **193**, 67-79. doi:10.1007/s00359-006-0171-0
Thomas, K. N., Gower, D. J., Bell, R. C., Fujita, M. K., Schott, R. K. and Streicher, J. W. (2020). Eye size and investment in frogs and toads correlate with adult habitat, activity pattern and breeding ecology. *Proc. R. Soc. B* **287**, 20201393. doi:10.1098/rspb.2020.1393
Ullmann, J. F. P., Moore, B. A., Temple, S. E., Fernández-Juricic, E. and Collin, S. P. (2012). The retinal wholemount technique: A window to understanding the brain and behaviour. *Brain Behav. Evol.* **79**, 26-44. doi:10.1159/000332802
Veilleux, C. C. and Kirk, E. C. (2014). Visual acuity in mammals: effects of eye size and ecology. *Brain Behav. Evol.* **83**, 43-53. doi:10.1159/000357830
Verbeek, B. (1972). Ethologische Untersuchungen an einigen europaischen Eidechsen. *Bonner Zool. Beitrage* **23**, 122-151.
Walls, G. L. (1942). *The Vertebrate Eye and Its Adaptive Radiation*. New York: Hafner.
Warrant, E., Johnsen, S. and Nilsson, D. E. (2020). Light and visual environments. In *The Senses: A Comprehensive Reference*, 2nd edn. (ed. B. Fritzsch), p. 126. University of Iowa, US, Academic Press.
Weber, H. (1957). Vergleichende Untersuchung des Verhaltens von Smaragdeidechsen (*Lacerta viridis*), Mauereidechsen (*L. muralis*) und Perleidechsen (*L. lepida*). *Z. Tierpsychol.* **14**, 448-472. doi:10.1111/j.1439-0310.1957.tb00548.x
West, M. J., Slomianka, L. and Gundersen, H. J. G. (1991). Unbiased stereological estimation of the total number of neurons in the subdivisions of the rat hippocampus using the optical fractionator. *Anat. Rec.* **231**, 482-497. doi:10.1002/ar.1092310411

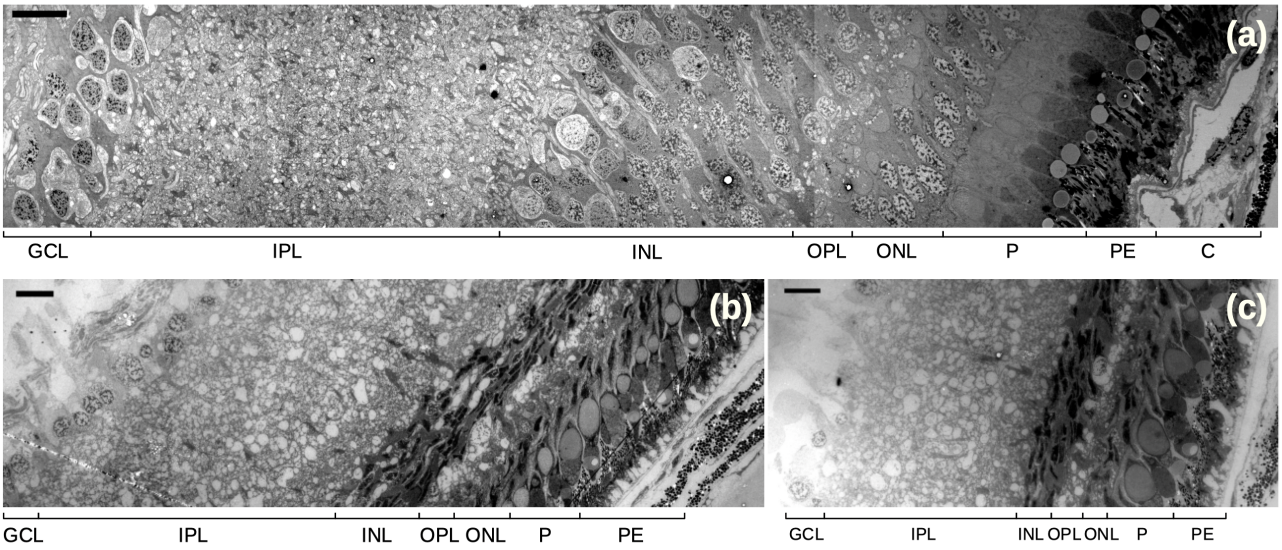

Fig. S1. Crossed sections of a retina of *Podarcis muralis* under Transmission Electron Microscopy (TEM) in (a) peak density area, (b) medium density area and (c) low density area in a peripheral region. Scale bars = 10 µm. **CP**: *Conus papillaris*, **R**: Retina, **ON**: Optic Nerve, **NFL**: Nerve Fibre Layer (axons), **GCL**: Ganglion Cell Layer, **IPL**: Inner Plexiform Layer, **INL**: Inner Nuclear Layer (amacrine, bipolar, and horizontal cells), **OPL**: Outer Plexiform Layer, **ONL**: Outer Nuclear Layer, **P**: Photoreceptors, **PE**: Pigmented Epithelium, **C**: Choroid.

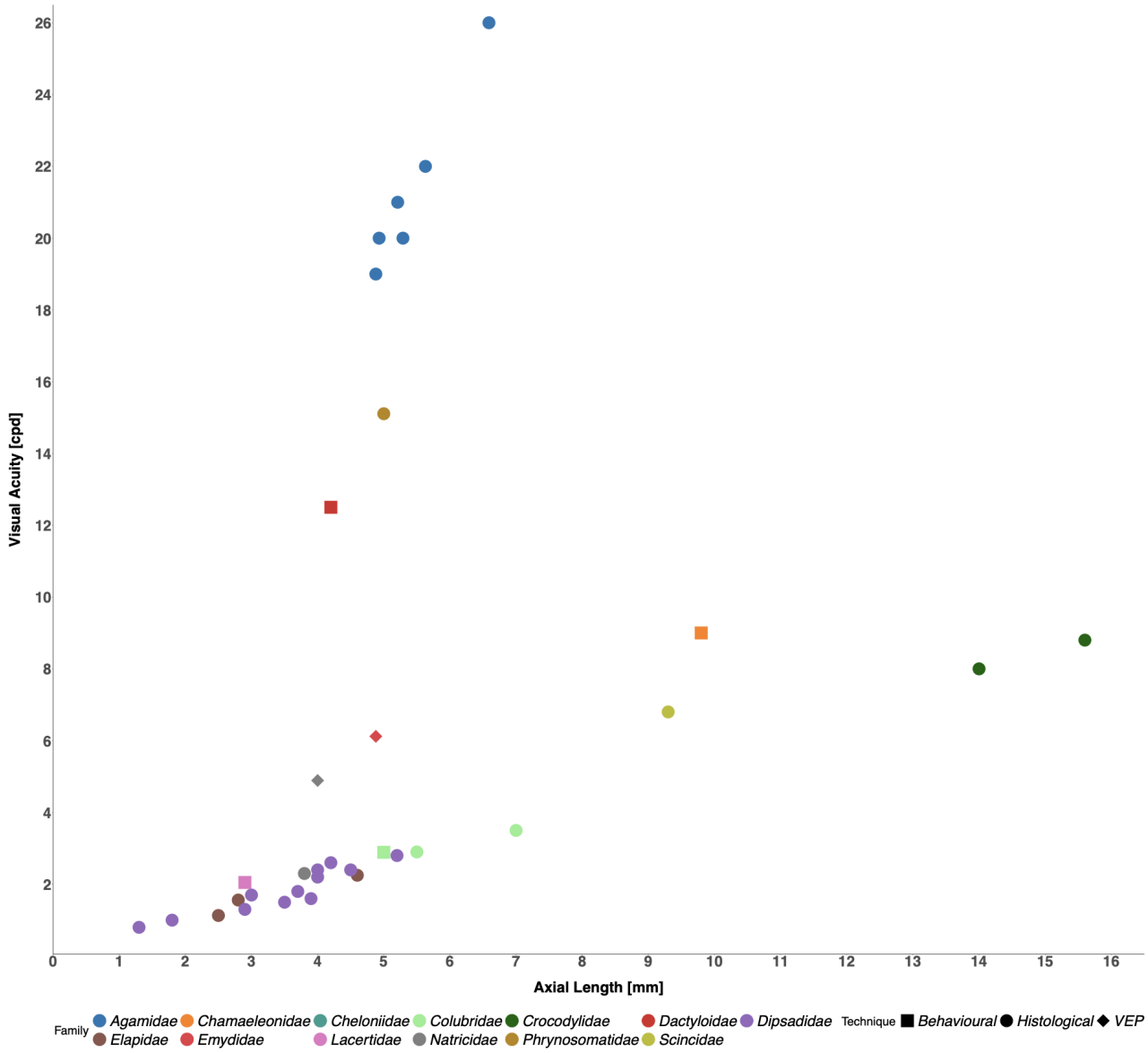

Fig. S2. Visual acuity (in cpd) relative to axial length (in mm) across different reptile families, using original estimates as directly reported in the literature. Acuity estimates were obtained using behavioural (square), histological (circle), or visual evoked potential (VEP; diamond) methods. Colours correspond to the different reptile families, as indicated in the legend. Table S1 of the Supplementary Information provides information on eye morphology and corresponding references for each species.

Table S1. Data used for Fig. 7

References	Order	Family	Species	Activity	Visual acuity [minute of arc]	Technique	Cited visual acuity [cpd]	Peak GCL [cells/mm2]	AL [mm]	PND [mm]	RMF*0.5	fN [cpd]
Hart et al., 2012	Squamata	Elapidae	*Aipysurus laevis*	nocturnal	NA	Histological	2.25	8400	4.6	2.62	0.0229	2.252
Makaretz & Levine, 1980; Fleishman, 1992; Fleishman et al., 2017	Squamata	Dactyloidae	*Anolis carolinensis*	diurnal	4.8	Behavioural & Histological	12.5 or 13.6	290000	4.2	2.8	0.0245	14.203
Fleishman et al., 2017	Squamata	Dactyloidae	*Anolis sagrei*	diurnal	NA	Behavioural	1.22 (periphery)	NA	4.5	3.02	0.0263	NA
Hauzman et al. 2018	Squamata	Dipsadidae	*Atractus pantostictus*	nocturnal	NA	Histological	0.8	16788	1.3	0.68	0.0059	0.821
Hauzman et al. 2018	Squamata	Dipsadidae	*Atractus reticulatus*	nocturnal	NA	Histological	1	11992	1.8	0.94	0.0082	0.961
Bartol et al. 2001; 2003	Testudines	Cheloniidae	*Caretta caretta*	diurnal	5.34 or 12.89	Behavioural	5.60	NA	18.8	12.6	0.1099	NA
Hassni et al., 1997; Lev-Ari et al., 2017; Ketter-Katz et al., 2020	Squamata	Chamaeleonidae	*Chamaeleo chamaeleon*	diurnal	NA	Behavioural & Histological	9	13200	9.8	6.57	0.0573	7.071
Hauzman et al., 2018	Squamata	Colubridae	*Chironius bicarinatus*	diurnal	NA	Histological	2.9	11623	5.5	2.86	0.0249	2.890
Zamore et al., 2020	Squamata	Colubridae	*Chrysopelea paradisi*	diurnal	NA	Behavioural	2.89	NA	5	2.6	0.0227	NA
Nagloo et al., 2016	Crocodilia	Crocodylidae	*Crocodylus johnstoni*	diurnal	NA	Histological	8	11375	14	7.98	0.0696	7.977
Nagloo et al., 2016	Crocodilia	Crocodylidae	*Crocodylus porosus*	diurnal	NA	Histological	8.8	11083	15.6	8.89	0.0776	8.774
Nagloo et al., 2019	Squamata	Agamidae	*Ctenophorus decresii*	diurnal	NA	Histological	20	80000	5.29	3.54	0.0309	9.396
Nagloo et al., 2019	Squamata	Agamidae	*Ctenophorus gibba*	diurnal	NA	Histological	22	83167	5.63	3.77	0.0329	10.196
Nagloo et al., 2019	Squamata	Agamidae	*Ctenophorus nuchalis*	diurnal	NA	Histological	26	78750	6.59	4.42	0.0385	11.613
Nagloo et al., 2019	Squamata	Agamidae	*Ctenophorus ornatus*	diurnal	NA	Histological	19	65000	4.88	3.27	0.0285	7.813
Nagloo et al., 2019	Squamata	Agamidae	*Ctenophorus pictus*	diurnal	NA	Histological	20	71667	4.93	3.3	0.0288	8.288
Nagloo et al., 2019	Squamata	Agamidae	*Ctenophorus vadnappa*	diurnal	NA	Histological	21	70000	5.21	3.49	0.0304	8.656
Hauzman et al., 2018	Squamata	Dipsadidae	*Dipsas albifrons*	nocturnal	NA	Histological	1.5	7933	3.5	1.82	0.0159	1.519
Hart et al., 2012	Squamata	Elapidae	*Disteira major*	diurnal	NA	Histological	1.13	7200	2.5	1.43	0.0124	1.133
Hauzman et al. 2018	Squamata	Dipsadidae	*Erythrolamprus aesculapii*	diurnal	NA	Histological	2.4	12176	4.5	2.34	0.0204	2.420
Hauzman et al. 2018	Squamata	Dipsadidae	*Erythrolamprus miliaris*	diurnal	NA	Histological	2.2	12281	4	2.08	0.0181	2.160
Hauzman et al., 2018	Squamata	Dipsadidae	*Erythrolamprus poecilogyrus*	diurnal	NA	Histological	1.7	13381	3	1.56	0.0136	1.691
Canei & Nonclercq, 2020	Squamata	Scincidae	*Eumeces schneideri*	diurnal	NA	Histological	NA	39489	5.28	3.77	0.0329	7.022

Supplementary Information

Hart et al., 2012	Squamata	Elapidae	*Hydrophis curtus*	diurnal	NA	Histological	1.56	10800	2.8	1.6	0.0139	1.555
Baker et al., 2007	Squamata	Natricidae	*Nerodia sipedon pleuralis*	diurnal	NA	VEP	4.89	NA	4	2.08	0.0234	NA
Hauzman et al., 2018	Squamata	Dipsadidae	*Oxyrhopus guibei*	nocturnal	NA	Histological	1.3	8798	2.9	1.51	0.0132	1.326
Hauzman et al., 2014	Squamata	Dipsadidae	*Philodryas olfersii*	diurnal	NA	Histological	2.6	15275	4.2	2.18	0.0190	2.530
Hauzman et al., 2014	Squamata	Dipsadidae	*Philodryas patagoniensis*	diurnal	NA	Histological	2.8	12009	5.2	2.7	0.0236	2.777
Hauzman et al., 2018	Squamata	Dipsadidae	*Pseudoboa neuwiedii*	nocturnal	NA	Histological	1.8	9531	3.7	1.92	0.0168	1.761
Ott et al., 2004	Squamata	Phrynosomatidae	*Phrynosoma cornutum*	diurnal	NA	Histological	15.11	NA	5	3	0.0175	NA
Canei et al., 2020	Squamata	Scincidae	*Scincus scincus*	diurnal	NA	Histological	NA	84449	3.85	2.79	0.0243	7.599
Hauzman et al., 2018	Squamata	Dipsadidae	*Sibynomorphus mikanii*	nocturnal	NA	Histological	1.6	7195	3.9	2.03	0.0177	1.612
Hauzman et al., 2018	Squamata	Colubridae	*Spilotes pullatus*	diurnal	NA	Histological	3.5	10815	7	3.64	0.0317	3.548
Guan et al., 2022	Testudines	Emydidae	*Terrapene carolina*	diurnal	NA	Behavioural	0.43	NA	NA	NA	NA	NA
Wong, 1989; Fontenot, 2008	Squamata	Natricidae	*Thamnophis sirtalis*	diurnal	NA	Histological	2.3	10000	3.8	2.55	0.0222	2.386
New & Bull, 2011	Squamata	Scincidae	*Tiliqua rugosa*	diurnal	NA	Histological	6.8	15500	9.3	6.25	0.0545	7.293
Hauzman et al., 2018	Squamata	Dipsadidae	*Tomodon dorsatus*	diurnal	NA	Histological	2.4	14759	4	2.08	0.0181	2.368
Northmore & Granda, 1991	Reptilia	Emydidae	*Trachemys scripta elegans*	diurnal	NA	VEP	6.12	NA	4.88	3.27	0.0285	NA
The present study	Squamata	Lacertidae	*Podarcis muralis*	diurnal	NA	Behavioural & Histological	2.05	7322	2.9	1.94	0.0169	1.558

AL: Axial Length, **f*N***: Nyquist limits of spatial resolution, **GC**: Ganglion Cell, **PND**: Post Nodal Distance, **RMF**: Retinal Magnification Factor, **VEP**: Visual Evoked Potential

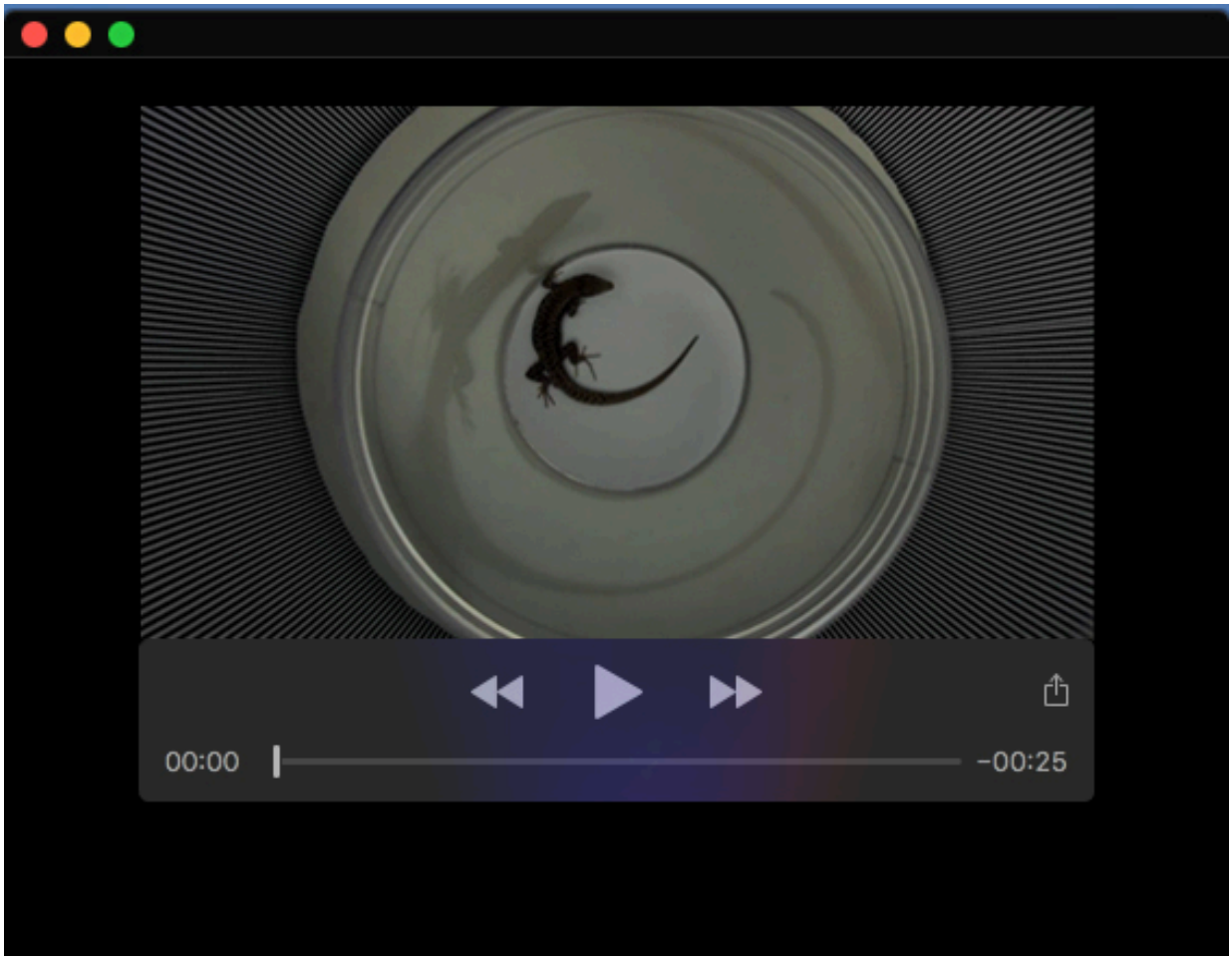

Movie 1. Representative video recording of a *Podarcis muralis* individual exhibiting an optomotor response (OMR) during an optomotor apparatus assay. The trial corresponds to a spatial frequency of 1 cycle per degree (cpd).

References

Baker, R. A., Gawne, T. J., Loop, M. S., and Pullman, S. (2007). Visual acuity of the midland banded water snake estimated from evoked telencephalic potentials. *Journal of Comparative Physiology A*, **193**(8), 865-870.

Bartol, S. M., and Musick, J. A. (2001). Morphology and topographical organization of the retina of juvenile loggerhead sea turtles (*Caretta caretta*). *Copeia*, **2001**(3), 718-725.

Bartol, S. M., Mellgren, R. L., and Musick, J. A. (2003). Visual acuity of juvenile loggerhead sea turtles (*Caretta caretta*): A behavioral approach. *International Journal of Comparative Psychology*, **16**(2), 143-155.

Canei, J., Burtea, C., and Nonclercq, D. (2020). Comparative study of the visual system of two psammophilic lizards (*Scincus scincus* & *Eumeces schneideri*). *Vision Research*, **171**, 17-30.

Fleishman, L. J. (1992). The influence of the sensory system and the environment on motion patterns in the visual displays of anoline lizards and other vertebrates. *The American Naturalist*, **139**, S36-S61.

Fleishman, L. J., Yeo, A. I., and Perez, C. W. (2017). Visual acuity and signal color pattern in an Anolis lizard. Journal of Experimental Biology, **220**(12), 2154-2158.

Fontenot, C. L. (2008). Variation in pupil diameter in North American Gartersnakes (*Thamnophis*) is regulated by immersion in water, not by light intensity. *Vision Research*, **48**(15), 1663-1669.

Guan, J., Cameron, D. J., and Eng, C. (2022). Quantifying visual acuity of *Terrapene carolina* triunguis utilizing optokinetic response. *Veterinary Ophthalmology*, **26**(3), 205-210.

Hart, N. S., Coimbra, J. P., Collin, S. P. and Westhoff, G. (2012). Photoreceptor types, visual pigments, and topographic specializations in the retinas of hydrophiid sea snakes. *Journal of Comparative Neurology*, **520**(6), 1246-1261.

Hassni, M. E., M'Hamed, S. B., Repérant, J., and Bennis, M. (1997). Quantitative and Topographical Study of Retinal Ganglion Cells in the Chameleon (*Chameleo chameleon*). *Brain Research Bulletin*, **44**(5), 621-625.

Hauzman, E., Bonci, D. M., Grotzner, S. R., Mela, M., Liber, A. M., Martins, S. L., and Ventura, D. F. (2014). Comparative study of photoreceptor and retinal ganglion cell topography and spatial resolving power in Dipsadidae snakes. *Brain Behavior and Evolution*, **84**(3), 197-213.

Hauzman, E., Bonci, D. M., and Ventura, D. F. (2018). Retinal topographic maps: a glimpse into the animals' visual world. *Sensory nervous system*, **1**, 101-126.

Ketter-Katz, H., Lev-Ari, T., and Katzir, G. (2020). Vision in chameleons - A model for non-mammalian vertebrates. *Seminars in Cell and Developmental Biology*, **106**, 94-105.

Lev-Ari, T., Katz, H. K., Lustig, A., and Katzir, G. (2017). Visual acuity and optokinetic directionality in the common chameleon (*Chamaeleo chamaeleon*). EC *Ophthalmology*, **6**(5), 145-154.

Makaretz, M., and Levine, R. L. (1980). A light microscopic study of the bifoveate retina in the lizard *Anolis carolinensis*: general observations and convergence ratios. *Vision Research*, **20**(8), 679-686.

Muramoto, C., Cardoso-Brito, V., Raposo, A. C., Torres Pires, T., and Pontes Oriá, A. (2020). Ocular ultrasonography of sea turtles. *Acta Veterinaria Scandinavica*, **62**, 52.

Nagloo, N., Collin, S. P., Hemmi, J. M., and Hart, N. S. (2016). Spatial resolving power and spectral sensitivity of the saltwater crocodile, *Crocodylus porosus*, and the freshwater crocodile, *Crocodylus johnstoni*. *Journal of Experimental Biology*, **219**(9), 1394-1404.

Nagloo, N., Coimbra, J. P., Hoops, D., Hart, N. S., Collin, S. P., and Hemmi, J. M. (2019). Retinal topography and microhabitat diversity in a group of dragon lizards. *Journal of Comparative Neurology*, **528**(4), 542-558.

New, S. T. D., and Bull, C. M. (2011). Retinal ganglion cell topography and visual acuity of the sleepy lizard (*Tiliqua rugosa*). *Journal of Comparative Physiology A*, **197**(6), 703-709.

Northmore, D. P. M., and Granda, A. M. (1991). Refractive state, contrast sensitivity, and resolution in the freshwater turtle, *Pseudemys scripta elegans*, determined by tectal visual-evoked potentials. *Visual neuroscience*, **7**(6), 619-625.

Ott, M., Ostheim, J., and Sherbrooke, W. C. (2004). Prey snapping and visual distance estimation in Texas horned lizards, *Phrynosoma cornutum*. *Journal of experimental biology*, **207**(17), 3067-3072.

Wong, R. O. (1989). Morphology and distribution of neurons in the retina of the American garter snake *Thamnophis sirtalis*. *Journal of Comparative Neurology*, **283**(4), 587-601.

Zamore, S. A., Araujo, N., and Socha, J. J. (2023). Visual acuity in the flying snake, *Chrysopelea paradisi*. *Integrative and Comparative Biology*, **63**(1), 209-222.